

LHC and lepton flavour violation phenomenology of a left-right extension of the MSSM

J.N. Esteves,^a J.C. Romao,^a M. Hirsch,^b A. Vicente,^b W. Porod^c and F. Staub^c

^a*Departamento de Física and CFTP, Instituto Superior Técnico,
Av. Rovisco Pais 1, 1049-001 Lisboa, Portugal*

^b*AHEP Group, Instituto de Física Corpuscular — C.S.I.C./Universitat de València,
Edificio de Institutos de Paterna, Apartado 22085, E-46071 València, Spain*

^c*Institut für Theoretische Physik und Astronomie, Universität Würzburg,
Am Hubland, 97074 Würzburg, Germany*

E-mail: joaomest@cftp.ist.utl.pt, jorge.romao@ist.utl.pt,
mahirsch@ific.uv.es, Avelino.Vicente@ific.uv.es,
porod@physik.uni-wuerzburg.de, florian.staub@physik.uni-wuerzburg.de

ABSTRACT: We study the phenomenology of a supersymmetric left-right model, assuming minimal supergravity boundary conditions. Both left-right and (B-L) symmetries are broken at an energy scale close to, but significantly below the GUT scale. Neutrino data is explained via a seesaw mechanism. We calculate the RGEs for superpotential and soft parameters complete at 2-loop order. At low energies lepton flavour violation (LFV) and small, but potentially measurable mass splittings in the charged scalar lepton sector appear, due to the RGE running. Different from the supersymmetric “pure seesaw” models, both, LFV and slepton mass splittings, occur not only in the left- but also in the right slepton sector. Especially, ratios of LFV slepton decays, such as $\text{Br}(\tilde{\tau}_R \rightarrow \mu\chi_1^0)/\text{Br}(\tilde{\tau}_L \rightarrow \mu\chi_1^0)$ are sensitive to the ratio of (B-L) and left-right symmetry breaking scales. Also the model predicts a polarization asymmetry of the outgoing positrons in the decay $\mu^+ \rightarrow e^+\gamma$, $\mathcal{A} \sim [0, 1]$, which differs from the pure seesaw “prediction” $\mathcal{A} = 1$. Observation of any of these signals allows to distinguish this model from any of the three standard, pure (mSugra) seesaw setups.

KEYWORDS: Supersymmetry Phenomenology

ARXIV EPRINT: [1011.0348](https://arxiv.org/abs/1011.0348)

Contents

1	Introduction	1
2	Left-right supersymmetric model	4
2.1	Step 1: From GUT scale to $SU(2)_R$ breaking scale	5
2.2	Step 2: From $SU(2)_R$ breaking scale to $U(1)_{B-L}$ breaking scale	7
2.3	Step 3: From $U(1)_{B-L}$ breaking scale to EW/SUSY scale	10
2.4	Neutrino masses, LFV and Yukawa couplings	11
2.5	Parameter counting	13
3	Numerical results	14
3.1	Procedure for numerics	14
3.2	Mass spectrum	15
3.3	LFV of leptons	16
3.4	LFV at LHC/ILC	23
4	Conclusions	29
A	RGEs	30
A.1	Calculation of supersymmetric RGEs	30
A.2	From GUT scale to $SU(2)_R$ breaking scale	32
A.2.1	Anomalous dimensions	32
A.2.2	Beta functions for soft breaking masses of sleptons	34
A.2.3	Beta functions for gauge couplings	34
A.3	From $SU(2)_R$ breaking scale to $U(1)_{B-L}$ breaking scale	34
A.3.1	Anomalous dimensions	34
A.3.2	Beta functions for soft breaking masses of sleptons	37
A.3.3	Beta functions for gauge couplings	37

1 Introduction

The most popular explanation for the observed smallness of neutrino masses is certainly the seesaw mechanism [1–6]. Literally hundreds of theoretical papers based on “the seesaw” have been published since the discovery of neutrino oscillations [7–9]. The seesaw can be implemented at tree-level in exactly three realizations [10]: exchange of a fermionic singlet, a.k.a. the right-handed neutrino (type-I) [1–4]; of a scalar triplet (type-II) [4–6]; or of a fermionic triplet (type-III) [11]. In any of these “seesaw mechanisms” neutrino masses are given by $m_\nu \sim v^2/\Lambda$, where v is the Higgs vacuum expectation value (vev) and Λ the scale of the seesaw. For coefficients $\mathcal{O}(1)$ and $\Lambda \sim (10^{14}–10^{15})$ GeV one finds neutrinos

with sub-eV masses, just as experimental data demands. Unfortunately, attractive as this idea might appear from the theoretical point of view, this estimate also implies that “the seesaw” will never be *directly* tested.

This situation might change slightly, if supersymmetry (SUSY) is found at the LHC, essentially because scalar leptons provide potentially additional information about seesaw parameters. Assuming SUSY gets broken at a high energy scale, the seesaw parameters leave their imprint on the soft parameters in the Renormalization Group Equation (RGE) running. Then, at least in principle, indirect tests of the seesaw become possible.¹ Indeed, this has been pointed out already in [12], where it was shown that lepton flavour violating (LFV) off-diagonal mass terms for sleptons are automatically generated in seesaw (type-I), even if SUSY breaking is completely flavour blind at the GUT scale as in minimal supergravity (mSugra).²

Motivated by the above arguments, many authors have then studied LFV in SUSY models. For the seesaw type-I, low energy LFV decays such as $l_i \rightarrow l_j \gamma$ and $l_i \rightarrow 3l_j$ have been calculated in [13–22]; $\mu-e$ conversion in nuclei has been studied in [23, 24]. The type-II seesaw has received much less attention, although it has actually fewer free parameters than type-I. The latter implies that ratios of LFV decays of leptons can actually be predicted as a function of neutrino angles in mSugra, as has been shown in [25, 26]. Finally, for completeness we mention that LFV in SUSY seesaw type-III has been studied in [27].

Measurements at colliders, once SUSY is discovered, can provide additional information. LFV decays of left sleptons within mSugra have been studied for type-I in [28] and for type-II in [26, 29]. Precise mass measurements might also show indirect effects of the seesaw [30–32]. Most prominently, type-II and type-III seesaw contain non-singlet superfields, so gauge couplings run differently from pure MSSM. One then expects that sparticle spectra show a characteristic “deformation” with respect to mSugra predictions. From different combinations of masses one can form “invariants”, i.e. numbers which to leading order depend only on the seesaw scale [33], although there are important corrections at 2-loop [26, 27], which have to be included before any quantitative analysis can be done. Experimentally interesting is also that at the LHC the mass splitting between selectrons and smuons may be constrained down to $\mathcal{O}(10^{-4})$ for 30 fb^{-1} of integrated luminosity [34]. In mSugra, one expects this splitting to be unmeasurably tiny, whereas in mSugra plus seesaw significantly different masses can be generated, as has been shown for type-I in [35].

Interestingly, in pure seesaw models with flavour blind SUSY boundary conditions all of the effects discussed above show up only in the left slepton sector. Naturally one expects that in a supersymmetric model with an intermediate left-right symmetric stage, also the right sleptons should contain some indirect information about the high energy parameters. This simple observation forms the main motivation for the current paper. Before entering in the details of our calculation, let us first briefly discuss left-right symmetric models.

¹In the general minimal supersymmetric extension of the standard model (MSSM) *all* soft terms are free parameters, fixed at the electroweak scale and nothing can be learned about the high energy world.

²It might be technically more correct to call this setup the “constrained MSSM” (CMSSM). We will stick to the terminology mSugra.

Quite a large number of different left-right (LR) symmetric models have been discussed in the literature. Originally LR models were introduced to explain the observed left-handedness of the weak interaction as a consequence of symmetry breaking [36–38]. However, LR models offer other advantages as well. First, the particle content of LR models contains automatically the right-handed neutrino and thus the ingredients for generating a (type-I) seesaw mechanism.³ Second, the gauge group $SU(3)_c \times SU(2)_L \times SU(2)_R \times U(1)_{B-L}$ is one of the possible chains through which $SO(10)$ [39, 40] can be broken to the standard model gauge group.⁴ In addition, it has been shown that they provide technical solutions to the SUSY CP and strong CP problems [41] and they give an understanding of the $U(1)$ charges of the standard model fermions. Interesting only for the supersymmetric versions of LR models, $(B-L)$ is gauged and thus, potentially, the low energy theory conserves R-parity [42, 43].

This last argument requires possibly some elaboration. R-parity, defined as $R_P = (-1)^{3(B-L)+2s}$ (where B and L stand for baryon and lepton numbers and s for the spin of the particle), is imposed in the MSSM to avoid dangerous baryon and lepton number violating operators. However, the origin of R_P is not explained within the MSSM. In early LR models $SU(2)_R$ doublets were used to break the gauge symmetry. The non-supersymmetric model proposed in references [37, 38] introduced two additional scalar doublets χ_L and χ_R , where $\chi_L \equiv \chi_L(1, 2, 1, 1)$ and $\chi_R \equiv \chi_R(1, 1, 2, -1)$ under $SU(3)_c \times SU(2)_L \times SU(2)_R \times U(1)_{B-L}$. Parity conservation implies that both, χ_L and χ_R , are needed. When the neutral component of χ_R gets a vev, $\langle \chi_R^0 \rangle \neq 0$, the gauge symmetry is broken down to the SM gauge group. However, χ_R is odd under $U(1)_{B-L}$ and thus, in the SUSY versions of this setup, R_P is broken at the same time.⁵ A possible solution to this problem is to break the gauge symmetry by $SU(2)_R$ fields with even charge under $U(1)_{B-L}$, i.e. by triplets. For a SUSY LR model, this was in fact proposed in reference [45], where four triplets were added to the MSSM spectrum: $\Delta(1, 3, 1, 2)$, $\Delta^c(1, 1, 3, -2)$, $\bar{\Delta}(1, 3, 1, -2)$ and $\bar{\Delta}^c(1, 1, 3, 2)$. Breaking the symmetry by the vev of Δ^c produces at the same time a right-handed neutrino mass via the operator $L^c \Delta^c L^c$, leading to a type-I seesaw mechanism. Depending on whether or not Δ gets a vev, also a type-II seesaw can be generated [46].

However, whether R-parity is conserved in this setup is not clear. The reason is that the minimum of the potential might prefer a solution in which also the right-handed scalar neutrino gets a vev, thus breaking R_P , as has been claimed to be the case in [47]. Later [48] calculated some 1-loop corrections to the scalar potential, concluding that R_P conserving minima can be found. On the other hand, as first noted in [49] and later showed by Aulakh and collaborators [50, 51], by the addition of two more triplets, $\Omega(1, 3, 1, 0)$ and $\Omega^c(1, 1, 3, 0)$, with zero lepton number one can achieve LR breaking with conserved R_P guaranteed already at tree-level. Lacking a general proof that the model [45] conserves R_P we will follow [50, 51] as the setup for our numerical calculations.

³Breaking the LR symmetry with triplets can generate also a type-II [4].

⁴Not all $SO(10)$ breaking chains contain a seesaw. Neither does $SU(5)$. It is, of course, straightforward to *add* a seesaw to $SU(5)$.

⁵This could be solved by imposing additional discrete symmetries on the model that forbid the dangerous \hat{R}_p operators [44], but this cannot be regarded as automatic R-parity conservation.

Finally, for completeness we mention the existence of left-right models with R-parity violation. For example, if the left-right symmetry is broken with the vevs of right-handed sneutrinos R-parity gets broken as well and the resulting phenomenology is totally different, as shown in [52, 53].

Compared to the long list of papers about indirect tests of the seesaw, surprisingly little work on the “low-energy” phenomenology of SUSY LR models has been done. One loop RGEs for two left-right SUSY models have been calculated in [54]. These two models are (with one additional singlet): (a) breaking LR by doublets a la [37, 38] and (b) by triplets following [45], but no numerical work at all was done in this paper. The possibility that right sleptons might have flavour violating decays in the left-right symmetric SUSY model of [45] was mentioned in [55]. A systematic study of all the possible signals discussed above for the seesaw case is lacking and to our knowledge there is no publication of any calculation of these signals for the model of [50, 51]. (For completeness we would like to mention that in GUTs based on SU(5) one can have the situation the LFV occurs *only* in the right slepton sector, as pointed out in [56]. However, this model [56] is in a different class from all the models discussed above, since it does not contain non-zero neutrino masses.)

The rest of this paper is organized as follows. In the next section we define the model [50, 51] and discuss its particle content and main features at each symmetry breaking scale. We have calculated the RGEs for each step complete at the 2-loop level following the general description by [57] using the Mathematica package SARAH [58–60]. A summary is given in the appendix, the complete set of equations and the SARAH model files can be found at [61]. Neutrino masses can be fitted to experimental data via a type-I seesaw mechanism and we discuss different ways to implement the fit. We then turn to the numerical results. The output of SARAH has been passed to the program package SPheno [62] for numerical evaluation. We calculate the SUSY spectra and LFV slepton decays, such as $\tilde{\tau}_{L/R} \rightarrow \mu \tilde{\chi}_1^0$ and $\tilde{\tau}_{L/R} \rightarrow e \tilde{\chi}_1^0$ and $\tilde{\chi}_2^0 \rightarrow e \mu \tilde{\chi}_1^0$, as well as low-energy decays $l_i \rightarrow l_j \gamma$ for some sample points as a function of the LR and (B-L) scales. Potentially measurable signals are found in both, left and right slepton sectors, if (a) the seesaw scale is above (very roughly) 10^{13} GeV and (b) if the scale of LR breaking is significantly below the GUT scale. Since we find sizable LFV soft masses in both slepton sectors, also the polarization in $\mu \rightarrow e \gamma$ is different from the pure seesaw expectation. We then close with a short summary and outlook.

2 Left-right supersymmetric model

In this section we define the model, its particle content and give a description of the different symmetry breaking steps. The fit to neutrino masses and its connection to LFV violation in the slepton sector is discussed in some detail, to prepare for the numerical results given in the next section. We summarize briefly the free parameters of the theory.

The model essentially follows [50, 51]. We have not attempted to find a GUT completion. We will, however, assume that gauge couplings and soft SUSY parameters can be unified, i.e. implicitly assume that such a GUT model can indeed be constructed.

Superfield	generations	SU(3) _c	SU(2) _L	SU(2) _R	U(1) _{B-L}
Q	3	3	2	1	$\frac{1}{3}$
Q^c	3	$\bar{3}$	1	2	$-\frac{1}{3}$
L	3	1	2	1	-1
L^c	3	1	1	2	1
Φ	2	1	2	2	0
Δ	1	1	3	1	2
$\bar{\Delta}$	1	1	3	1	-2
Δ^c	1	1	1	3	-2
$\bar{\Delta}^c$	1	1	1	3	2
Ω	1	1	3	1	0
Ω^c	1	1	1	3	0

Table 1. Matter content between the GUT scale and the SU(2)_R breaking scale.

2.1 Step 1: From GUT scale to SU(2)_R breaking scale

Just below the GUT scale the gauge group of the model is SU(3)_c × SU(2)_L × SU(2)_R × U(1)_{B-L}. In addition it is assumed that parity is conserved, see below. The matter content of the model is given in table 1. Here Q , Q^c , L and L^c are the quark and lepton superfields of the MSSM with the addition of (three) right-handed neutrino(s) ν^c .

Two Φ superfields, bidoublets under SU(2)_L × SU(2)_R, are introduced. They contain the standard H_d and H_u MSSM Higgs doublets. In this model, two copies are needed for a non-trivial CKM matrix. Although there are known attempts to build a realistic LR model with only one bidoublet generating the quark mixing angles at the loop level [63], we will not rely on such a mechanism. Finally, the rest of the superfields in table 1 are introduced to break the LR symmetry, as explained above.

Table 1 shows also the gauge charges for the matter content in the model. In particular, the last column shows the $B - L$ value for the different superfields. However, the following definition for the electric charge operator will be used throughout this paper

$$Q = I_{3L} + I_{3R} + \frac{B - L}{2} \tag{2.1}$$

and thus the U(1)_{B-L} charge is actually $\frac{B-L}{2}$.

With the representations in table 1, the most general superpotential compatible with the gauge symmetry and parity is

$$\begin{aligned} \mathcal{W} = & Y_Q Q \Phi Q^c + Y_L L \Phi L^c - \frac{\mu}{2} \Phi \Phi + f L \Delta L + f^* L^c \Delta^c L^c \\ & + a \Delta \Omega \bar{\Delta} + a^* \Delta^c \Omega^c \bar{\Delta}^c + \alpha \Omega \Phi \Phi + \alpha^* \Omega^c \Phi \Phi \\ & + M_\Delta \Delta \bar{\Delta} + M_\Delta^* \Delta^c \bar{\Delta}^c + M_\Omega \Omega \Omega + M_\Omega^* \Omega^c \Omega^c . \end{aligned} \tag{2.2}$$

Note that this superpotential is invariant under the parity transformations $Q \leftrightarrow (Q^c)^*$, $L \leftrightarrow (L^c)^*$, $\Phi \leftrightarrow \Phi^\dagger$, $\Delta \leftrightarrow (\Delta^c)^*$, $\bar{\Delta} \leftrightarrow (\bar{\Delta}^c)^*$, $\Omega \leftrightarrow (\Omega^c)^*$. This discrete symmetry fixes,

for example, the $L^c \Delta^c L^c$ coupling to be f^* , the complex conjugate of the $L \Delta L$ coupling, thus reducing the number of free parameters of the model.

Family and gauge indices have been omitted in eq. (2.2), more detailed expressions can be found in [50]. Y_Q and Y_L are quark and lepton Yukawa couplings. However, with two bidoublets there are two copies of them, and thus there are four 3×3 Yukawa matrices. Conservation of parity implies that they must be hermitian. μ is a 2×2 symmetric matrix, whose entries have dimensions of mass, f is a 3×3 (dimensionless) complex symmetric matrix, and α is a 2×2 antisymmetric matrix, and thus it only contains one (dimensionless) complex parameter, α_{12} . The mass parameters M_Ω and M_Δ can be exchanged for v_R and v_{BL} , the vacuum expectation values of the scalar fields that break the LR symmetry, see below.

The soft terms of the model are

$$\begin{aligned}
 -\mathcal{L}_{\text{soft}} = & m_Q^2 \tilde{Q}^\dagger \tilde{Q} + m_{Q^c}^2 \tilde{Q}^{c\dagger} \tilde{Q}^c + m_L^2 \tilde{L}^\dagger \tilde{L} + m_{L^c}^2 \tilde{L}^{c\dagger} \tilde{L}^c \\
 & + m_\Phi^2 \Phi^\dagger \Phi + m_\Delta^2 \Delta^\dagger \Delta + m_{\bar{\Delta}}^2 \bar{\Delta}^\dagger \bar{\Delta} + m_{\Delta^c}^2 \Delta^{c\dagger} \Delta^c + m_{\bar{\Delta}^c}^2 \bar{\Delta}^{c\dagger} \bar{\Delta}^c \\
 & + m_\Omega^2 \Omega^\dagger \Omega + m_{\Omega^c}^2 \Omega^{c\dagger} \Omega^c + \frac{1}{2} [M_1 \tilde{B}^0 \tilde{B}^0 + M_2 (\tilde{W}_L \tilde{W}_L + \tilde{W}_R \tilde{W}_R) + M_3 \tilde{g} \tilde{g} + h.c.] \\
 & + [T_Q \tilde{Q} \tilde{\Phi} \tilde{Q}^c + T_L \tilde{L} \tilde{\Phi} \tilde{L}^c + T_f \tilde{L} \Delta \tilde{L} + T_f^* \tilde{L}^c \Delta^c \tilde{L}^c \\
 & + T_a \Delta \Omega \bar{\Delta} + T_a^* \Delta^c \Omega^c \bar{\Delta}^c + T_\alpha \Omega \Phi \Phi + T_\alpha^* \Omega^c \Phi \Phi + h.c.] \\
 & + [B_\mu \Phi \Phi + B_{M_\Delta} \Delta \bar{\Delta} + B_{M_\Delta}^* \Delta^c \bar{\Delta}^c + B_{M_\Omega} \Omega \Omega + B_{M_\Omega}^* \Omega^c \Omega^c + h.c.] . \quad (2.3)
 \end{aligned}$$

Again, family and gauge indices have been omitted for the sake of simplicity. The LR model itself does not, of course, fix the values of the soft SUSY breaking terms. In the numerical evaluation of the RGEs we will resort to mSugra-like boundary conditions, i.e. $m_0^2 \mathcal{I}_{3 \times 3} = m_Q^2 = m_{Q^c}^2 = m_L^2 = m_{L^c}^2$, $m_0^2 \mathcal{I}_{2 \times 2} = m_\Phi^2$, $m_0^2 = m_\Delta^2 = m_{\bar{\Delta}}^2 = m_{\Delta^c}^2 = m_{\bar{\Delta}^c}^2 = m_\Omega^2 = m_{\Omega^c}^2$, $M_{1/2} = M_1 = M_2 = M_3$, $T_Q = A_0 Y_Q$, $T_L = A_0 Y_L$, $T_f = A_0 f$, $T_a = A_0 a$, $T_\alpha = A_0 \alpha$, $B_\mu = B_0$, $B_{M_\Delta} = B_0 M_\Delta$, $B_{M_\Omega} = B_0 M_\Omega$. The superpotential couplings f , Y_Q and Y_L are fixed by the low-scale fermion masses and mixing angles. Their values at the GUT scale are obtained by RGE running. This will be discussed in more detail in section 2.4.

The breaking of the LR gauge group to the MSSM gauge group takes place in two steps: $SU(2)_R \times U(1)_{B-L} \rightarrow U(1)_R \times U(1)_{B-L} \rightarrow U(1)_Y$. In the first step the neutral component of the triplet Ω takes a vev:

$$\langle \Omega^{c0} \rangle = \frac{v_R}{\sqrt{2}} \quad (2.4)$$

which breaks $SU(2)_R$. However, since $I_{3R}(\Omega^{c0}) = 0$ there is a $U(1)_R$ symmetry left over. Next, the group $U(1)_R \times U(1)_{B-L}$ is broken by

$$\langle \Delta^{c0} \rangle = \frac{v_{BL}}{\sqrt{2}}, \quad \langle \bar{\Delta}^{c0} \rangle = \frac{\bar{v}_{BL}}{\sqrt{2}} . \quad (2.5)$$

The remaining symmetry is now $U(1)_Y$ with hypercharge defined as $Y = I_{3R} + \frac{B-L}{2}$.

The tadpole equations do not link Ω^c , Δ^c and $\bar{\Delta}^c$ with their left-handed counterparts, due to supersymmetry. Thus, the left-handed triplets can have vanishing vevs [50] and the model produces only a type-I seesaw.

Superfield	generations	SU(3) _c	SU(2) _L	U(1) _R	U(1) _{B-L}
Q	3	3	2	0	$\frac{1}{3}$
d^c	3	$\bar{3}$	1	$\frac{1}{2}$	$-\frac{1}{3}$
u^c	3	$\bar{3}$	1	$-\frac{1}{2}$	$-\frac{1}{3}$
L	3	1	2	0	-1
e^c	3	1	1	$\frac{1}{2}$	1
ν^c	3	1	1	$-\frac{1}{2}$	1
H_d	1	1	2	$-\frac{1}{2}$	0
H_u	1	1	2	$\frac{1}{2}$	0
Δ^{c0}	1	1	1	1	-2
$\bar{\Delta}^{c0}$	1	1	1	-1	2
Ω	1	1	3	0	0
Ω^{c0}	1	1	1	0	0

Table 2. Matter content from the SU(2)_R breaking scale to the U(1)_{B-L} breaking scale.

Although a “hierarchy” between the two breaking scales may exist, $v_{BL} \ll v_R$, one cannot neglect the effects of the second breaking stage on the first one, since mass terms of Ω and Δ enter in both tadpole equations. If we assume $\bar{v}_{BL} = v_{BL}$ the tadpole equations of the model can be written

$$\frac{\partial V}{\partial v_R} = 4|M_\Omega|^2 v_R + \frac{1}{2}|a|^2 v_{BL}^2 v_R - \frac{1}{2} v_{BL}^2 [a^*(M_\Delta + M_\Omega) + c.c] = 0, \quad (2.6)$$

$$\frac{\partial V}{\partial v_{BL}} = |M_\Delta|^2 v_{BL} + \frac{1}{4}|a|^2 (v_{BL}^2 + v_R^2) v_{BL} - \frac{1}{2} v_{BL} v_R [a^*(M_\Delta + M_\Omega) + c.c] = 0. \quad (2.7)$$

In these equations (small) soft SUSY breaking terms have been neglected. Similarly, at this stage there are no electroweak symmetry breaking vevs v_d and v_u . From equations (2.6) and (2.7) one sees that, in fact, there is an inverse hierarchy between the vevs and the superpotential masses M_Δ , M_Ω , given by

$$v_R = \frac{2M_\Delta}{a}, \quad v_{BL} = \frac{2}{a} (2M_\Delta M_\Omega)^{1/2}. \quad (2.8)$$

And so, $v_{BL} \ll v_R$ requires $M_\Delta \gg M_\Omega$, as has already been discussed in [50].

2.2 Step 2: From SU(2)_R breaking scale to U(1)_{B-L} breaking scale

At this step the gauge group is SU(3)_c × SU(2)_L × U(1)_R × U(1)_{B-L}. The particle content of the model from the SU(2)_R breaking scale to the U(1)_{B-L} breaking scale is given in table 2.

Some comments might be in order. Despite M_Δ being of the order of v_R (or larger), see eq.(2.8), not all components of the Δ superfields receive large masses. The neutral components of Δ^c and $\bar{\Delta}^c$ lie at the v_{BL} scale. One can easily check that the F-term contributions to their masses vanish in the minimum of the scalar potential eq. (2.8).

Moreover, Ω^c does not generate D-terms contributions to their masses. Therefore, contrary to the other components of the Δ triplets, they only get masses at the v_{BL} scale. On the other hand, one might guess that all components in the Ω, Ω^c superfields should be retained at this stage, since their superpotential mass M_Ω is required to be below v_{BL} . However, some of their components get contributions from $SU(2)_R$ breaking, and thus they become heavy. The charged components of Ω^c do develop large masses, in the case of the scalars through D-terms, while in the case of the fermions due to their mixing with the charged gauginos \tilde{W}_R^\pm , which have masses proportional to v_R . However, the neutral components of Ω^c do not get $SU(2)_R$ breaking contributions, since they have $I_{3R}(\Omega^{c0}) = 0$, and then they must be included in this energy regime. See reference [51] for a more quantitative discussion.

After $SU(2)_R$ breaking the two bidoublets Φ_1 and Φ_2 get split into four $SU(2)_L$ doublets. Two of them must remain light, identified with the two Higgs doublets of the MSSM, responsible for EW symmetry breaking, while, at the same time, the other two get masses of the order of v_R . This strong hierarchy can be only obtained by imposing a fine-tuning condition on the parameters involved in the bidoublet sector.

The superpotential terms mixing the four $SU(2)_L$ doublets can be rewritten as

$$\mathcal{W}_M = (H_d^f)^T M_H H_u^f \tag{2.9}$$

where $H_d^f = (H_d^1, H_d^2)$ and $H_u^f = (H_u^1, H_u^2)$ are the *flavour eigenstates*. In this basis reads the matrix

$$M_H = \begin{pmatrix} \mu_{11} & \mu_{12} + \alpha_{12} M_R \\ \mu_{12} - \alpha_{12} M_R & \mu_{22} \end{pmatrix}, \tag{2.10}$$

where the relations $\mu_{ij} = \mu_{ji}$ and $\alpha_{ij} = -\alpha_{ji}$ have been used and $M_R = \frac{v_R}{2}$ has been defined. In order to get two light doublets we impose the fine-tuning condition [51]

$$\text{Det}(M_H) = \mu_{11}\mu_{22} - (\mu_{12}^2 - \alpha_{12}^2 M_R^2) = 0. \tag{2.11}$$

The result of eq. (2.11) is to split the two Higgs bidoublets into two pairs of doublets $(H_d, H_u)_L$ and $(H_d, H_u)_R$, where $(H_d, H_u)_L$ is the light pair that appears in table 2, and $(H_d, H_u)_R$ a heavy pair with mass of order of v_R . In practice, equation (2.11) implies that one of the superpotential parameters must be chosen in terms of the others. Since this fine-tuning condition is not protected by any symmetry, the RGEs do not preserve it, and one must impose it at the $SU(2)_R$ breaking scale. In our computation we chose to compute μ_{11} in terms of the free parameters μ_{12} , μ_{22} , α_{12} and v_R .

In order to compute the resulting couplings for the light Higgs doublets one must rotate the original fields into their mass basis. Since M_H is not a symmetric matrix (unless $\alpha_{12} = 0$) one has to rotate independently H_d^f and H_u^f , i.e. $H_d^f = D H_d^m$, $H_u^f = U H_u^m$, where D and U are orthogonal matrices and $H_d^m = (H_d^L, H_d^R)$ and $H_u^m = (H_u^L, H_u^R)$ are the *mass eigenstates*. This way one finds

$$\mathcal{W}_M = (H_d^f)^T M_H H_u^f = (H_d^m)^T D^T M_H U H_u^m = (H_d^m)^T \hat{M}_H H_u^m \tag{2.12}$$

where \hat{M}_H is a diagonal matrix, with eigenvalues

$$\begin{aligned}\hat{M}_{H,1}^2 &= 0, \\ \hat{M}_{H,2}^2 &= \frac{1}{\mu_{22}^2} (\alpha_{12}^4 M_R^4 + 2\alpha_{12}^2 M_R^2 (\mu_{22}^2 - \mu_{12}^2) + (\mu_{22}^2 + \mu_{12}^2)^2). \end{aligned} \quad (2.13)$$

The D and U rotations are, in general, different and we parametrize them as

$$D = \begin{pmatrix} \cos \theta_1 & \sin \theta_1 \\ -\sin \theta_1 & \cos \theta_1 \end{pmatrix}, \quad U = \begin{pmatrix} \cos \theta_2 & \sin \theta_2 \\ -\sin \theta_2 & \cos \theta_2 \end{pmatrix} \quad (2.14)$$

and get

$$\begin{aligned}H_d^1 &= \cos \theta_1 H_d^L + \sin \theta_1 H_d^R, \\ H_d^2 &= -\sin \theta_1 H_d^L + \cos \theta_1 H_d^R, \end{aligned} \quad (2.15)$$

and similar for H_u . In general the angles θ_1 and θ_2 are different. However, they are connected to the same matrix M_H and can be calculated by diagonalizing $M_H(M_H)^T$ or $(M_H)^T M_H$ and one finds

$$\tan \theta_{1,2} = \frac{\mu_{12} \pm \alpha_{12} M_R}{\mu_{22}}. \quad (2.16)$$

In these expressions $\text{Det}(M_H) = 0$ has been used to simplify the result. Exact $\text{Det}(M_H) = 0$ implies that the μ -term of the MSSM is zero, so this condition can only be true up to small corrections, see the discussion below. Note that there are two interesting limits. First, $\mu_{12} \gg \alpha_{12} M_R$: this implies $\tan \theta_1 = \tan \theta_2$ and therefore $D = U$. This is as expected, since that limit makes M_H symmetric. And, second, $\mu_{12} \ll \alpha_{12} M_R$: this implies $\tan \theta_1 = -\tan \theta_2$ and therefore $D = U^T$.

The superpotential at this stage is

$$\begin{aligned}\mathcal{W} &= Y_u Q H_u u^c + Y_d Q H_d d^c + Y_e L H_d e^c + Y_\nu L H_u \nu^c + \mu H_u H_d \\ &+ f_c^1 \nu^c \nu^c \Delta^{c0} + M_{\Delta^c}^1 \Delta^{c0} \bar{\Delta}^{c0} + a_c^1 \Delta^{c0} \bar{\Delta}^{c0} \Omega^{c0} \\ &+ b \Omega H_d H_u + b_c \Omega^{c0} H_d H_u + M_\Omega \Omega \Omega + M_{\Omega^c} \Omega^{c0} \Omega^{c0}. \end{aligned} \quad (2.17)$$

Particles belonging to the same $SU(2)_R$ gauge multiplets split due to their different $U(1)_R$ charges. At this stage both the LR group, that symmetrizes the $SU(2)_L$ and $SU(2)_R$ gauge interactions, and the discrete parity symmetry that we imposed on the couplings are broken.

The soft terms are

$$\begin{aligned}-\mathcal{L}_{\text{soft}} &= m_Q^2 \tilde{Q}^\dagger \tilde{Q} + m_{u^c}^2 \tilde{u}^{c\dagger} \tilde{u}^c + m_{d^c}^2 \tilde{d}^{c\dagger} \tilde{d}^c + m_L^2 \tilde{L}^\dagger \tilde{L} + m_{e^c}^2 \tilde{e}^{c\dagger} \tilde{e}^c + m_{\nu^c}^2 \tilde{\nu}^{c\dagger} \tilde{\nu}^c \\ &+ m_{H_u}^2 H_u^\dagger H_u + m_{H_d}^2 H_d^\dagger H_d + m_{\Delta^{c0}}^2 \Delta^{c0\dagger} \Delta^{c0} + m_{\bar{\Delta}^{c0}}^2 \bar{\Delta}^{c0\dagger} \bar{\Delta}^{c0} \\ &+ m_\Omega^2 \Omega^\dagger \Omega + m_{\Omega^{c0}}^2 \Omega^{c0\dagger} \Omega^{c0} + \frac{1}{2} [M_1 \tilde{B}^0 \tilde{B}^0 + M_L \tilde{W}_L \tilde{W}_L + M_R \tilde{W}_R^0 \tilde{W}_R^0 + M_3 \tilde{g} \tilde{g} + h.c.] \\ &+ [T_u \tilde{Q} H_u \tilde{u}^c + T_d \tilde{Q} H_d \tilde{d}^c + T_e \tilde{L} H_d \tilde{e}^c + T_\nu \tilde{L} H_u \tilde{\nu}^c] \end{aligned} \quad (2.18)$$

$$\begin{aligned}
 &+T_{f_c}^1 \tilde{\nu}^c \tilde{\nu}^c \Delta^{c0} + T_{a_c}^1 \Delta^{c0} \Omega^{c0} \bar{\Delta}^{c0} + T_b \Omega H_d H_u + T_{b^c} \Omega^{c0} H_d H_u + h.c.] \\
 &+ [B_\mu H_u H_d + B_{M_{\Delta^c}^1} \Delta^{c0} \bar{\Delta}^{c0} + B_{M_\Omega} \Omega \Omega + B_{M_\Omega^c} \Omega^{c0} \Omega^{c0} + h.c.] .
 \end{aligned}$$

Again we suppress gauge and family indices.

We must impose matching conditions at the $SU(2)_R$ breaking scale. These are for superpotential parameters given by

$$\begin{aligned}
 Y_d &= Y_Q^1 \cos \theta_1 - Y_Q^2 \sin \theta_1, & Y_u &= -Y_Q^1 \cos \theta_2 + Y_Q^2 \sin \theta_2, \\
 Y_e &= Y_L^1 \cos \theta_1 - Y_L^2 \sin \theta_1, & Y_\nu &= -Y_L^1 \cos \theta_2 + Y_L^2 \sin \theta_2, \\
 f_c^1 &= -f^*, & a_c^1 &= -\frac{a^*}{\sqrt{2}}, \\
 M_{\Delta^c}^1 &= M_{\Delta^*}, & M_{\Omega^c} &= M_{\Omega^*}, \\
 b &= 2\alpha R, & b_c &= \sqrt{2}\alpha^* R,
 \end{aligned} \tag{2.19}$$

where $R = \sin(\theta_1 - \theta_2)$. For the soft masses we have

$$\begin{aligned}
 m_{u^c}^2 &= m_{d^c}^2 = m_{Q^c}^2, & (2.20) \\
 m_{e^c}^2 &= m_{\nu^c}^2 = m_{L^c}^2, \\
 m_{\Delta^{c0}}^2 &= m_{\Delta^c}^2, \\
 m_{\bar{\Delta}^{c0}}^2 &= m_{\bar{\Delta}^c}^2, \\
 m_{\Omega^{c0}}^2 &= m_{\Omega^c}^2, \\
 M_L &= M_R = M_2.
 \end{aligned}$$

Soft trilinears matching follow corresponding conditions. In addition, one has

$$\begin{aligned}
 m_{H_d}^2 &= \cos^2 \theta_1 (m_{\Phi}^2)_{11} + \sin^2 \theta_1 (m_{\Phi}^2)_{22} - \sin \theta_1 \cos \theta_1 [(m_{\Phi}^2)_{12} + (m_{\Phi}^2)_{21}], \\
 m_{H_u}^2 &= \cos^2 \theta_2 (m_{\Phi}^2)_{11} + \sin^2 \theta_2 (m_{\Phi}^2)_{22} - \sin \theta_2 \cos \theta_2 [(m_{\Phi}^2)_{12} + (m_{\Phi}^2)_{21}],
 \end{aligned}$$

as obtained when the operator $m_{\Phi}^2 \Phi^\dagger \Phi$ is projected into the light Higgs doublets operators $(H_d^L)^\dagger H_d^L$ and $(H_u^L)^\dagger H_u^L$. Gauge couplings are matched as $g_L = g_R = g_2$.

2.3 Step 3: From $U(1)_{B-L}$ breaking scale to EW/SUSY scale

We mention this stage only for completeness, since the last regime is just the usual MSSM. We need matching conditions in the gauge sector. Since $U(1)_R \times U(1)_{B-L}$ breaks to $U(1)_Y$, the MSSM gauge coupling g_1 will be a combination of g_R and g_{BL} . The resulting relationship is

$$g_1 = \frac{\sqrt{5} g_R g_{BL}}{\sqrt{2g_R^2 + 3g_{BL}^2}}. \tag{2.21}$$

Analogously, the following condition holds for gaugino masses

$$M_1(\text{MSSM}) = \frac{2g_R^2 M_1 + 3g_{BL}^2 M_R}{2g_R^2 + 3g_{BL}^2}. \tag{2.22}$$

parameter	best fit	2- σ
$\Delta m_{21}^2 [10^{-5} \text{eV}^2]$	$7.59_{-0.18}^{+0.23}$	7.22 – 8.03
$ \Delta m_{31}^2 [10^{-3} \text{eV}^2]$	$2.40_{-0.11}^{+0.12}$	2.18 – 2.64
$\sin^2 \theta_{12}$	$0.318_{-0.016}^{+0.019}$	0.29 – 0.36
$\sin^2 \theta_{23}$	$0.50_{-0.06}^{+0.07}$	0.39 – 0.63
$\sin^2 \theta_{13}$	$0.013_{-0.009}^{+0.013}$	≤ 0.039

Table 3. Best-fit values with 1- σ errors and 2- σ intervals (1 d.o.f.) taken from the reference [64], which is updated continuously on the web.

Note that in the last two equations the gauge couplings are GUT-normalized. Electroweak symmetry breaking occurs as in the MSSM. We take the Higgs doublet vevs

$$\langle H_d^0 \rangle = \frac{v_d}{\sqrt{2}}, \quad \langle H_u^0 \rangle = \frac{v_u}{\sqrt{2}}, \quad (2.23)$$

as free parameters and then solve the tadpole equations to find μ_{MSSM} and B^μ . μ_{MSSM} must be different from zero, that is $\text{Det}(M_H)$ can not be exactly zero. Instead the tuning must be exact up to $\text{Det}(M_H) = \mathcal{O}(\mu_{\text{MSSM}}^2)$. As usual $\tan \beta = \frac{v_u}{v_d}$ is used as a free parameter. Also the sign of μ_{MSSM} is not constrained as usual.

2.4 Neutrino masses, LFV and Yukawa couplings

Neutrino masses are generated after $U(1)_{B-L}$ breaking through a type-I seesaw mechanism. The matrix f_c^1 leads to Majorana masses for the right-handed neutrinos once Δ^{c0} gets a vev. We define the seesaw scale as the lightest eigenvalue of

$$M_S \equiv f_c^1 v_{\text{BL}}. \quad (2.24)$$

As usual, we can always rotate the fields to a basis where M_S is diagonal. However, this will introduce lepton flavour violating entries in the Y_{L_i} Yukawas, see discussion below. As mentioned above, contrary to non-supersymmetric LR models [4], there is no type-II contribution to neutrino masses.

Global fits to all available experimental data provide values for the parameters involved in neutrino oscillations, see table 3 for updated results and ref. [65, 66] for experimental results. As first observed in [67], these data imply that the neutrino mass matrix can be diagonalized to a good approximation by the so-called tri-bimaximal mixing pattern:

$$U_{\text{TBM}} = \begin{pmatrix} \sqrt{\frac{2}{3}} & \sqrt{\frac{1}{3}} & 0 \\ -\frac{1}{\sqrt{6}} & \frac{1}{\sqrt{3}} & -\frac{1}{\sqrt{2}} \\ -\frac{1}{\sqrt{6}} & \frac{1}{\sqrt{3}} & \frac{1}{\sqrt{2}} \end{pmatrix}. \quad (2.25)$$

The matrix product $Y_\nu \cdot (f_c^1)^{-1} \cdot Y_\nu^T$ is constrained by this particular structure. LFV entries can be present in both Y_ν and f_c^1 , see also the discussion about parameter counting in the next subsection. However, in the numerical section we will consider only two specific kinds of fits:

- Y_ν -fit: flavour structure in Y_ν and diagonal f_c^1 .
- f -fit: flavour structure in f_c^1 and diagonal Y_ν .

While at first it may seem either way of doing the fit is equivalent, f_c^1 and Y_ν in our setup can leave different traces in the soft slepton mass parameters if $v_{BL} \ll v_R$. This last condition is essential to distinguish between both possibilities, because otherwise one obtains the straightforward prediction that LFV entries in left and right slepton are equal, due to the assumed LR symmetry above v_R .

These two types of fit were already discussed in reference [68], which investigates low energy LFV signatures in a supersymmetric seesaw model where the right-handed neutrino mass is generated from a term of the form $f\Delta^c\nu^c\nu^c$. When the scalar component of Δ^c acquires a vev a type-I seesaw is obtained, generating masses for the light neutrinos. Therefore, this model has the ingredients to accommodate a Y_ν -fit, named as *Dirac LFV* in [68], or a f -fit, named as *Majorana LFV*. Note, however, that the left-right symmetry, central in our work, is missing in this reference, thus implying different signatures at the electroweak scale.

The difference in phenomenology of the two fits can be easily understood considering approximated expressions for the RGEs for m_L^2 and $m_{e^c}^2$. In the first step, from the GUT scale to the v_R scale RGEs at 1-loop order can be written in leading-log approximation as [55]

$$\begin{aligned} \Delta m_L^2 &= -\frac{1}{4\pi^2} \left(3ff^\dagger + Y_L^{(k)} Y_L^{(k)\dagger} \right) (3m_0^2 + A_0^2) \ln \left(\frac{m_{GUT}}{v_R} \right), \\ \Delta m_{L^c}^2 &= -\frac{1}{4\pi^2} \left(3f^\dagger f + Y_L^{(k)\dagger} Y_L^{(k)} \right) (3m_0^2 + A_0^2) \ln \left(\frac{m_{GUT}}{v_R} \right). \end{aligned} \quad (2.26)$$

Of course, also the A parameters develop LFV off-diagonals in the running. We do not give the corresponding approximated equations for brevity. After parity breaking at the v_R scale the Yukawa coupling Y_L splits into Y_e , the charged lepton Yukawa, and Y_ν , the neutrino Yukawa. The later contributes to LFV entries in the running down to the v_{BL} scale. Thus,

$$\begin{aligned} \Delta m_L^2 &\sim -\frac{1}{8\pi^2} Y_\nu Y_\nu^\dagger (3m_L^2|_{v_R} + A_e^2|_{v_R}) \ln \left(\frac{v_R}{v_{BL}} \right), \\ \Delta m_{e^c}^2 &\sim 0, \end{aligned} \quad (2.27)$$

where $m_L^2|_{v_R}$ is the matrix m_L^2 at the scale v_R and $A_e^2|_{v_R}$ is defined as $T_e = Y_e A_e$ and also has to be taken at v_R . In order to understand the main difference between the two fits, let us first consider the f -fit. This assumes that Y_ν is diagonal at the seesaw scale and thus the observed low energy mismatch between the neutrino and charged lepton sectors is due to a non-trivial flavour structure in f_c^1 . Of course, non-diagonal entries in f generate in the running also non-diagonal entries in Y_ν and Y_e , but these can be neglected in first approximation. In this case, equations (2.26) and (2.27) show that the LR symmetry makes m_L^2 and $m_{e^c}^2$ run with the same flavour structure and the magnitudes of their off-diagonal entries at the SUSY scale are similar. If, on the other hand, Y_ν is non-trivial (Y_ν -fit), while

f is diagonal, the running from the GUT scale to the v_R scale induces again the same off-diagonal entries in m_L^2 and m_{Lc}^2 . However, from v_R to v_{BL} the off-diagonal entries in m_L^2 continue to run, while those in m_{Lc}^2 do not. This effect, generated by the right-handed neutrinos via the Y_ν Yukawas, induces additional flavour violating effects in the L sector compared to the R sector. Seeing LFV in both left and right slepton sectors thus allows us to indirectly learn about the high energy theory. We will study this in some detail in the numerical section below.

2.5 Parameter counting

Let us briefly summarize the free parameters of the model. With the assumption of mSugra (or better: mSugra-like) boundary conditions, in the SUSY breaking sector we only have the standard parameters $m_0, M_{1/2}, A_0, \tan \beta, \text{sign}(\mu_{\text{MSSM}})$. Thus, we count 4+1 parameters in the soft terms. We note in passing that the soft terms of the heavy sector, of course, do not have to follow strictly the conditions outlined in equation (2.3), as long as these parameters are small compared to v_{BL} there are no changes compared to the above discussion.

In the superpotential we have a, α, μ, M_Δ and M_Ω . This leaves, at first sight, 7 parameters free. However, we can reduce them to 4+2 parameters as follows. Since $\alpha_{ij} = -\alpha_{ji}$, α only contains one free parameter: α_{12} . The matrix μ has 3 entries, but one of them, μ_{11} , is fixed by the fine-tuning condition $\text{Det}(M_H) = \mathcal{O}(\mu_{\text{MSSM}}^2)$. This leaves two free parameters, μ_{12}, μ_{22} . We have traded M_Δ and M_Ω for the vevs v_R, v_{BL} , since $\ln(\frac{v_R}{v_{BL}})$ and $\ln(\frac{v_{\text{GUT}}}{v_R})$ enter into the RGEs and thus can, at least in principle, be determined from low-energy spectra. There are then in summary 6 parameters, four independent of low-energy constraints and two which could be fixed from LFV data, see below.

In addition, in the superpotential we have the Yukawa matrices Y_{Q_i}, Y_{L_i} and f . Let's consider the quark sector first. Since we can always go to a basis in which one of the Y_{Q_i} is diagonal with only real entries, there are 12 parameters. Ten of them are fixed by six quark masses, three CKM angles and the CKM phase, leaving two phases undetermined.

In the lepton sector we have the symmetric matrices, Y_{L_1} and Y_{L_2} . As with the quark sector, a basis change shows that there are only 12 free parameters. f is symmetric and thus counts as another 9 parameters. Going to a basis in which f is diagonal does not reduce the number of free parameters, since in this basis we can no longer assume one of the Y_{L_i} to be diagonal. In summary there are thus free 21 parameters in these three matrices.

In the simple, pure seesaw type-I with three generations of right-handed neutrinos the number of free parameters is 21. Only 12 of them can be fixed from low-energy data: three neutrino and three charged lepton masses, three leptonic mixing angles and three phases (two Majorana and one Dirac phase). However, as pointed out in [15], in principle, m_L^2 contains 9 observable entries and thus, if the normalization (i.e. $m_0, A_0, \tan \beta$ etc.) is known from other sfermion measurements, one could re-construct the type-I seesaw parameters.⁶

How does the SUSY LR model compare to this? We have, as discussed above, also 21 parameters in the three coupling matrices, but neutrino masses depend also on v_{BL} .

⁶Of course, this discussion is slightly academic, since at least one of the Majorana phases will never be measured in praxis.

However, in principle, we have 9 more observables in $m_{\tilde{e}c}^2$, assuming again that the soft SUSY breaking terms can be extracted from other measurements. Since in the RGEs also v_R appears we have in total 23 parameters which need to be determined. The number of observables, on the other hand is fixed to 30 in total, as we have 12 (low-energy lepton sector) plus 9 (left sleptons) plus 9 (right sleptons) possible measurements.

3 Numerical results

3.1 Procedure for numerics

All necessary, analytical expressions were calculated with SARAH. For this purpose, two different model files for the model above the two threshold scales were created and used to calculate the full set of 2-loop RGEs. SARAH calculates the RGEs using the generic expressions of [57] in the most general form respecting the complete flavour structure. These RGEs were afterwards exported to Fortran code and implemented in SPheno. As starting point for the RGE running, the gauge and Yukawa couplings at the electroweak scale are used. In the calculation of the gauge and Yukawa couplings we follow closely the procedure described in ref. [62]: the values for the Yukawa couplings giving mass to the SM fermions and the gauge couplings are determined at the scale M_Z based on the measured values for the quark, lepton and vector boson masses as well as for the gauge couplings. Here, we have included the 1-loop corrections to the mass of W- and Z-boson as well as the SUSY contributions to δ_{v_B} for calculating the gauge couplings. Similarly, we have included the complete 1-loop corrections to the self-energies of SM fermions [69]. Moreover, we have resummed the $\tan\beta$ enhanced terms for the calculation of the Yukawa couplings of the b -quark and the τ -lepton as in [62]. The vacuum expectation values v_d and v_u are calculated with respect to the given value of $\tan\beta$ at M_Z . Since we are working with two distinct threshold scales, not all heavy fields are integrated out at their mass and the corresponding 1-loop boundary conditions at the threshold scales are needed. It is known that these particles cause a finite shift in the gauge couplings and gaugino masses. The general expressions are [70]

$$g_i \rightarrow g_i \left(1 \pm \frac{1}{16\pi^2} g_i^2 I_2^i(r) \ln \left(\frac{M^2}{M_T^2} \right) \right), \quad (3.1)$$

$$M_i \rightarrow M_i \left(1 \pm \frac{1}{16\pi^2} g_i^2 I_2^i(r) \ln \left(\frac{M^2}{M_T^2} \right) \right). \quad (3.2)$$

$I_2^i(r)$ is the Dynkin index of a field transforming as representation r with respect to the gauge group belonging to the gauge coupling g_i , M is the mass of this particle and M_T is the threshold scale. When evaluating the RGEs from the low to the high scale, the contribution is positive, when running down, it is negative. The different masses used for calculating the finite shifts are the eigenvalues of the full tree-level mass matrix of the charged, heavy particles removed from the spectrum. The correct mass spectrum is calculated in an iterative way. The GUT scale is defined as the scale at which $g_{BL} = g_2 = g_{GUT}$ holds. Generally, there is difference with g_3 to g_{GUT} in the percent range, the actual numerical mismatch depending on the scales v_{BL} and v_R and being larger for lower values

of v_{BL} and v_R . It has been stressed in particular in [71] that within supersymmetric LR models, the LR symmetry breaking scale has to be close to the GUT scale, otherwise this mismatch will grow too large. However, several solutions are known. In [72] it was pointed out that GUT thresholds - unknown unless the GUT model, including the complete Higgs sector used to break the GUT symmetry, is specified - can lead to important corrections, accounting for this apparent non-unification (for a discussion of these effects in the context of SU(5) see [73]). Another possibility is the addition of new particles to the spectrum. For example, reference [74] pointed out that new coloured superfields, charged under SU(3)_c but singlet under the other gauge subgroups, can easily lead to gauge coupling unification. Nevertheless, we simply use $g_{\text{BL}} = g_2 = g_{\text{GUT}}$ and attribute departures from complete unification to (unknown) thresholds and/or the existence of additional coloured particles below m_{GUT} . After applying the GUT scale boundary conditions, the RGEs are evaluated down to the low scale and the mass spectrum of the MSSM is calculated. The MSSM masses are, in general, calculated at the 1-loop level in the $\overline{\text{DR}}$ scheme using on-shell external momenta. For the Higgs fields also the most important 2-loop contributions are taken into account. We note that the corresponding Fortran routines are also written by SARAH but they are equivalent to the routines included in the public version of SPheno based on [69]. The iteration stops when the largest change in the calculation of the SUSY and Higgs boson masses at m_{SUSY} is below one per-mille between two iterations.

3.2 Mass spectrum

The appearance of charged particles at scales between the electroweak scale and the GUT scale leads to changes in the beta functions of the gauge couplings [25, 33]. This does not only change the evolution of the gauge couplings but also the evolution of the gaugino and scalar mass parameters [26, 33]. The LR model contains additional triplets, and similar to what is observed in the seesaw models [27] the mass spectrum at low energies is shifted with respect to mSugra expectations. Two examples of this behaviour are shown in figure 1. In this figure we show the two lightest neutralino masses and the masses of the left and right smuons versus v_{BL} (left side) and v_R (right side). We note that also all other sfermion and gaugino masses show the same dependence and in general smaller values are obtained for lower values of v_{BL} and v_R . One finds that gaugino masses depend stronger on v_{BL} and v_R than sfermion masses and that right sleptons are the sfermions for which the sensitivity to these vevs is smallest.

The change in the low energy spectrum, however, maintains to a good degree the standard mSugra expectation for the ratios of gaugino masses, as shown in figures 2 and 3. Here, figure 2 shows the ratios M_1/M_2 and M_2/M_3 versus v_{BL} , while figure 3 shows the same ratios versus v_R . Shown are the results for three different SUSY points, which in the limit of $v_R, v_{\text{BL}} \rightarrow m_{\text{GUT}}$ approach the standard SPS points SPS1a' [75], SPS3 and SPS5 [76]. For example, the ratio M_1/M_2 is expected to be $(5/3) \tan^2 \theta_W \simeq 0.5$ at 1-loop order in mSugra. The exact ratio, however, depends on higher order corrections, and thus on the SUSY spectrum. The LR model will thus appear rather mSugra like, if these ratios are measured. Only with very high precision on mass measurements, possible only at a linear collider, can one hope to find any (indirect) dependence on v_{BL} and v_R .

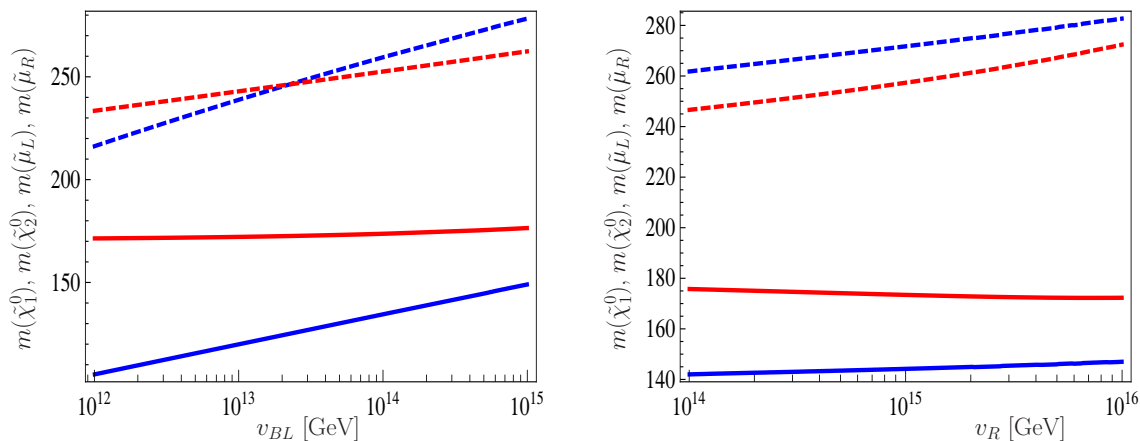


Figure 1. Example of spectra at the SUSY scale and its dependence on v_{BL} (left side) and v_R (right side). The masses of four states are shown: $\tilde{\chi}_1^0$ (blue line), $\tilde{\chi}_2^0$ (blue dashed line), $\tilde{\mu}_R$ (red line) and $\tilde{\mu}_L$ (red dashed line). In both panels the mSugra parameters have been taken as in the SPS3 benchmark point.

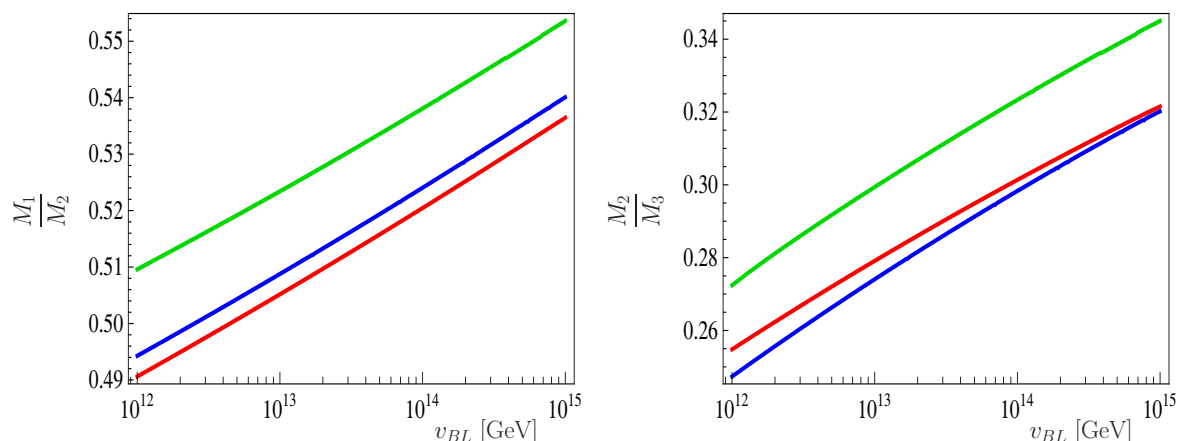


Figure 2. Gaugino mass ratios as a function of v_{BL} for the fixed value $v_R = 10^{15}$ GeV. To the left, M_1/M_2 , whereas to the right M_2/M_3 . In both figures the three coloured lines correspond to three mSugra benchmark points: SPS1a' (blue), SPS3 (green) and SPS5 (red). Note the small variation in the numbers on the Y axis.

3.3 LFV of leptons

Lepton flavour violation in charged lepton decays has attracted a lot of attention for decades. Processes like $\mu \rightarrow e\gamma$ are highly suppressed in the standard model (plus non-zero neutrino masses) due to the GIM mechanism [77], and thus the observation of these rare decays would imply new physics. The MEG experiment [78]⁷ is currently the most

⁷Documents and status at <http://meg.web.psi.ch/>, for a status report see for example [79].

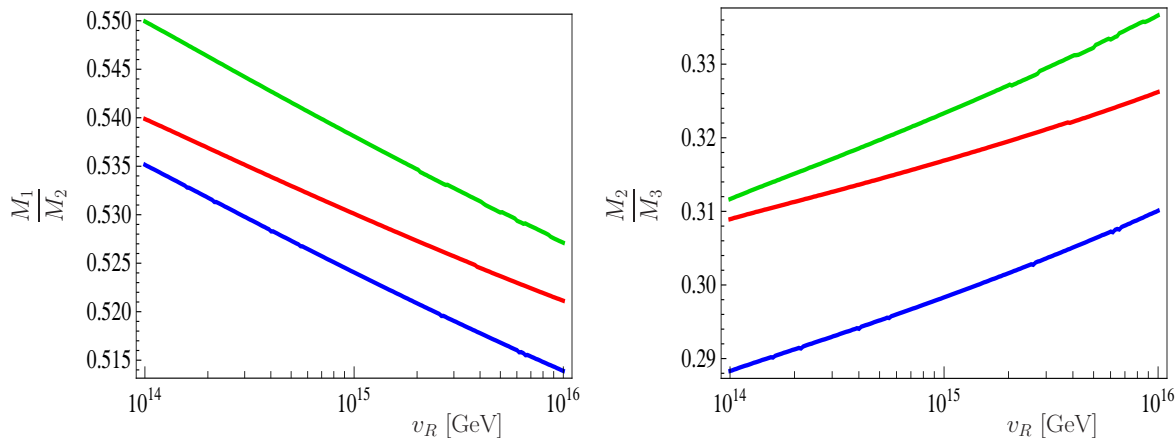


Figure 3. Gaugino mass ratios as a function of v_R for the fixed value $v_{BL} = 10^{14}$ GeV. To the left, M_1/M_2 , whereas to the right M_2/M_3 . In both figures the three coloured lines correspond to three mSugra benchmark points: SPS1a' (blue), SPS3 (green) and SPS5 (red). Note the small variation in the numbers on the Y axis.

advanced experimental setup in the search for $\mu^+ \rightarrow e^+\gamma$. This rare decay will be observed if its branching ratio is above the MEG expected sensitivity, around $Br(\mu \rightarrow e\gamma) \sim 10^{-13}$.

LFV decays like $l_i \rightarrow l_j\gamma$ are induced by 1-loop diagrams with the exchange of neutralinos and sleptons. They can be described by the effective Lagrangian, see for example the review [80],

$$\mathcal{L}_{\text{eff}} = e \frac{m_i}{2} \bar{l}_i \sigma_{\mu\nu} F^{\mu\nu} (A_L^{ij} P_L + A_R^{ij} P_R) l_j + h.c. . \quad (3.3)$$

Here $P_{L,R} = \frac{1}{2}(1 \mp \gamma_5)$ are the usual chirality projectors and therefore the couplings A_L and A_R are generated by loops with left and right sleptons, respectively. In our numerical calculation we use exact expressions for A_L and A_R . However, for an easier understanding of the numerical results, we note that the relation between these couplings and the slepton soft masses is very approximately given by

$$A_L^{ij} \sim \frac{(m_L^2)_{ij}}{m_{\text{SUSY}}^4}, \quad A_R^{ij} \sim \frac{(m_{ec}^2)_{ij}}{m_{\text{SUSY}}^4}, \quad (3.4)$$

where m_{SUSY} is a typical supersymmetric mass. Here it has been assumed that (a) chargino/neutralino masses are similar to slepton masses and (b) A-terms mixing left-right transitions are negligible. Therefore, due to the negligible off-diagonal entries in m_{ec}^2 , a pure seesaw model predicts $A_R \simeq 0$.

The branching ratio for $l_i \rightarrow l_j\gamma$ can be calculated from the previous formulas. The result is

$$Br(l_i \rightarrow l_j\gamma) = \frac{48\pi^3\alpha}{G_F^2} \left(|A_L^{ij}|^2 + |A_R^{ij}|^2 \right) Br(l_i \rightarrow l_j\nu_i\bar{\nu}_j) . \quad (3.5)$$

Figure 4 shows two examples for $Br(\mu \rightarrow e\gamma)$ in the $m_0, M_{1/2}$ plane. Here, we have fixed $v_{BL} = 10^{14}$ GeV and $v_R = 10^{15}$ GeV and show to the left $M_S = 10^{12}$ GeV, whereas

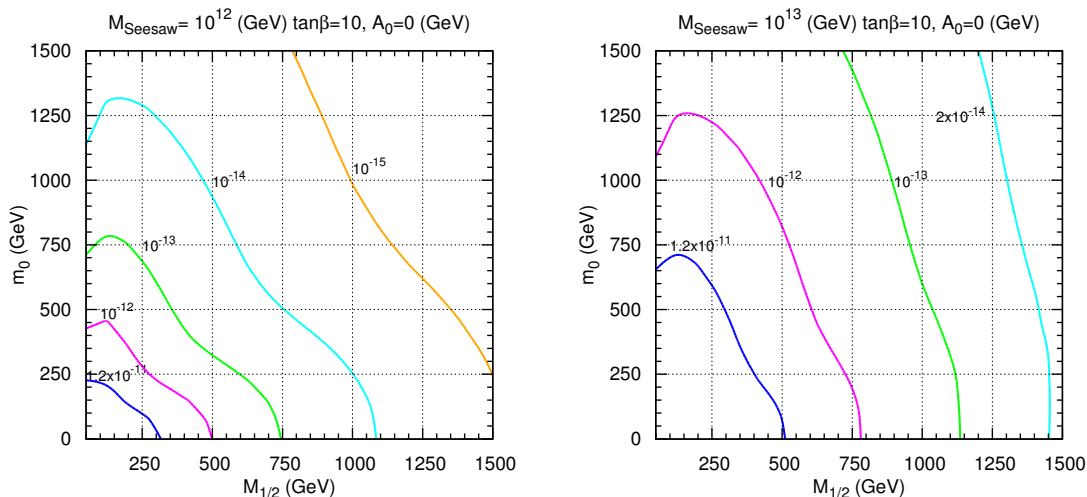


Figure 4. Contours of $Br(\mu \rightarrow e\gamma)$ in the $m_0, M_{1/2}$ plane for $v_{BL} = 10^{14}$ GeV and $v_R = 10^{15}$ GeV. To the left $M_S = 10^{12}$ GeV, whereas to the right $M_S = 10^{13}$ GeV. Neutrino oscillation data have been fitted with the Y_ν fit.

to the right $M_S = 10^{13}$ GeV. Here we have assumed a degenerate spectrum right-handed neutrinos which we denote by $M_S = M_{Ri}$. Once Yukawas are fitted to explain the observed neutrino masses, the branching ratio shows an approximately quadratic dependence on the seesaw scale, with lower M_S giving smaller $Br(\mu \rightarrow e\gamma)$. As expected, the branching ratio also strongly decreases as m_0 and/or $M_{1/2}$ increase. This is because the superparticles in the loops leading to $\mu \rightarrow e\gamma$ become heavier in these directions, suppressing the decay rate. In fact, from equations (3.4) and (3.5) one easily finds the dependence

$$Br(\mu \rightarrow e\gamma) \sim \frac{48\pi^3\alpha}{G_F^2} \frac{(m_{L,\bar{e}c}^2)_{ij}^2}{m_{\text{SUSY}}^8}, \quad (3.6)$$

which shows that $Br(\mu \rightarrow e\gamma)$ decreases as m_{SUSY}^{-8} .

It is also remarkable that for a given seesaw scale, $Br(\mu \rightarrow e\gamma)$ is sizeably larger in the LR model than in a pure seesaw type-I model, see for example [29]. The explanation of this is that right sleptons contribute significantly in the LR model to $Br(\mu \rightarrow e\gamma)$ and these contributions are absent in seesaw models.

As already discussed, a pure seesaw model predicts simply $A_R \simeq 0$. However, in the LR model we expect a more complicated picture. Left-right symmetry implies that, above the parity breaking scale, non-negligible flavour violating entries are generated in $m_{\bar{e}c}^2$. Therefore, $A_R \neq 0$ is obtained at low energy. The angular distribution of the outgoing positron at, for example, the MEG experiment could be used to discriminate between left- and right-handed polarized states [81, 82]. If MEG is able to measure the positron polarization asymmetry, defined as

$$\mathcal{A}(\mu^+ \rightarrow e^+\gamma) = \frac{|A_L|^2 - |A_R|^2}{|A_L|^2 + |A_R|^2}, \quad (3.7)$$

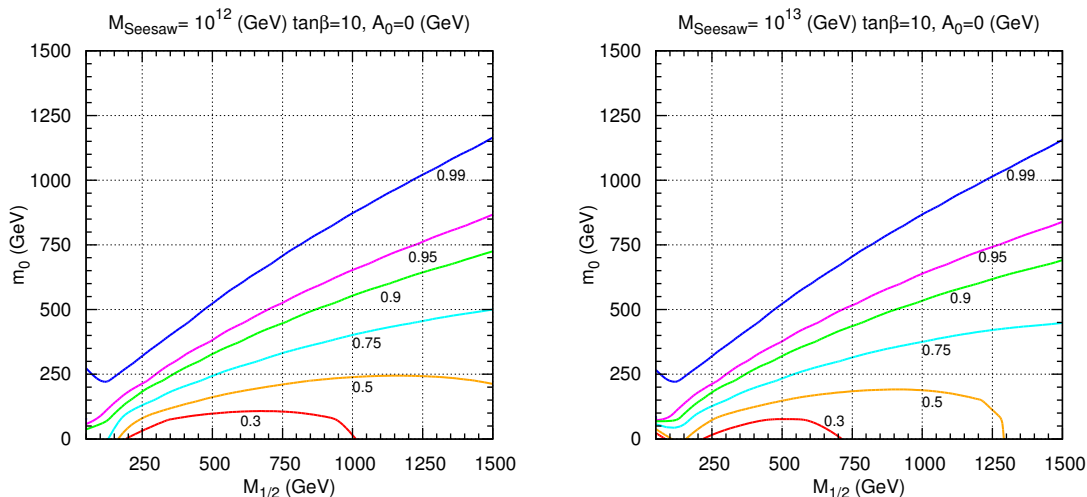


Figure 5. Contours of $\mathcal{A}(\mu^+ \rightarrow e^+\gamma)$ in the $m_0, M_{1/2}$ plane. To the left $M_S = 10^{12}$ GeV, whereas to the right $M_S = 10^{13}$ GeV. The parameters have been chosen as in figure 4.

there will be an additional observable to distinguish from minimal seesaw models. In a pure seesaw model one expects $\mathcal{A} \simeq +1$ to a very good accuracy. However, the LR model typically leads to significant departures from this expectation, giving an interesting signature of the high energy restoration of parity.

Figure 5 shows contours for $\mathcal{A}(\mu^+ \rightarrow e^+\gamma)$ in the $m_0, M_{1/2}$ plane. For the corresponding branching ratios see figure 4. Note the rather strong dependence on m_0 . The latter can be understood as follows. Since v_{BL} in these examples is one order of magnitude smaller than v_R , and the Y_ν fit has been used, the LFV mixing angles in the left slepton sector are larger than the corresponding LFV entries in the right sleptons. At very large values of m_0 , were the masses of right and left sleptons are of comparable magnitude, therefore “left” LFV is more important and the model approaches the pure seesaw expectation. At smaller values of m_0 , right sleptons are lighter than left sleptons, and due to the strong dependence of $\mu \rightarrow e\gamma$ on the sfermion masses entering the loop calculation, see eq. (3.4), A_R and A_L can become comparable, despite the smaller LFV entries in right slepton mass matrices. In the limit of very small right slepton masses the model then approaches $\mathcal{A} \sim 0$. We have not explicitly searched for regions of parameter space with $\mathcal{A} < 0$, but one expects that negative values for \mathcal{A} are possible if v_{BL} is not much below v_R and sleptons are light at the same time, i.e. small values of m_0 and $M_{1/2}$. Note that, again due to the LR symmetry above to v_R , the model can never approach the limit $\mathcal{A} = -1$ exactly.

The positron polarization asymmetry is very sensitive to the high energy scales. Figure 6 shows \mathcal{A} as a function of v_R for $M_S = 10^{13}$ GeV, $v_{BL} = 10^{14}$ GeV and the mSUGRA parameters as in the SPS3 benchmark point. The plot has been obtained using the Y_ν fit. This example shows that as v_R approaches m_{GUT} the positron polarization \mathcal{A} approaches +1, which means A_L dominates the calculation. This is because, in the Y_ν fit, the right-

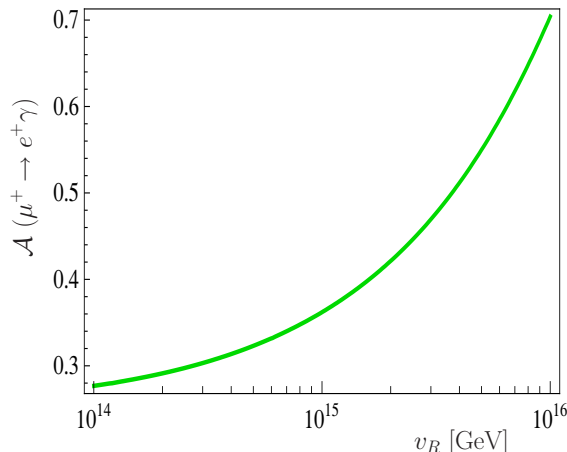


Figure 6. Positron polarization asymmetry $\mathcal{A}(\mu^+ \rightarrow e^+\gamma)$ as a function of v_R for the parameter choice $M_S = 10^{13}$ GeV and $v_{BL} = 10^{14}$ GeV. The mSugra parameters have been taken as in the SPS3 benchmark point and neutrino oscillation data have been fitted with the Y_ν fit, assuming degenerate right-handed neutrinos.

handed LFV soft slepton masses, and thus the corresponding A_R coupling, only run from m_{GUT} to v_R .

$\mathcal{A}(\mu^+ \rightarrow e^+\gamma)$ also has an important dependence on the seesaw scale. This is shown in figure 7, where \mathcal{A} is plotted as a function of the lightest right-handed neutrino mass. This dependence can be easily understood from the seesaw formula for neutrino masses. It implies that larger M_S requires larger Yukawa parameters in order to fit neutrino masses which, in turn, leads to larger flavour violating soft terms due to RGE running. However, note that, for very small seesaw scales all lepton flavour violating effects are negligible and no asymmetry is produced, since $A_L \sim A_R \sim 0$.

In addition, figure 7 shows again the relevance of v_R , which determines the parity breaking scale at which the LFV entries in the right-handed slepton sector essentially stop running. Lighter colours indicate larger v_R . As shown already in figure 6 for a particular point, the positron polarization approaches +1 as v_R is increased.

Below the $SU(2)_R$ breaking scale parity is broken and left and right slepton soft masses evolve differently. The approximate solutions to the RGEs in equations (2.26) and (2.27) show that, if neutrino data is fitted according to the Y_ν fit, the left-handed ones keep running from the $SU(2)_R$ breaking scale to the $U(1)_{B-L}$ scale. In this case one expects larger flavour violating effects in the left-handed slepton sector and a correlation with the ratio v_{BL}/v_R , which measures the difference between the breaking scales. This correlation, only present in the Y_ν fit, is shown in figure 8. On the one hand, one finds that as v_{BL} and v_R become very different, $v_{BL}/v_R \ll 1$, the positron asymmetry approaches $\mathcal{A} = +1$. On the other hand, when the two breaking scales are close, $v_{BL}/v_R \sim 1$, this effect disappears and the positron polarization asymmetry approaches $\mathcal{A} = 0$. Note that the Y_ν fit does not usually produce a negative value for \mathcal{A} since the LFV terms in the right slepton sector never run

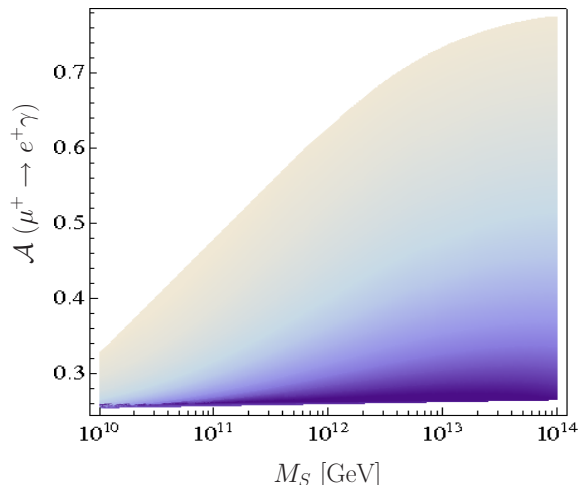


Figure 7. Positron polarization asymmetry $\mathcal{A}(\mu^+ \rightarrow e^+\gamma)$ as a function of the seesaw scale, defined as the mass of the lightest right-handed neutrino, for the parameter choice $v_{\text{BL}} = 10^{15}$ GeV and $v_R \in [10^{15}, 10^{16}]$ GeV. Lighter colours mean higher values of v_R . The mSugra parameters have been taken as in the SPS3 benchmark point and neutrino oscillation data have been fitted with the Y_ν fit, assuming degenerate right-handed neutrinos.

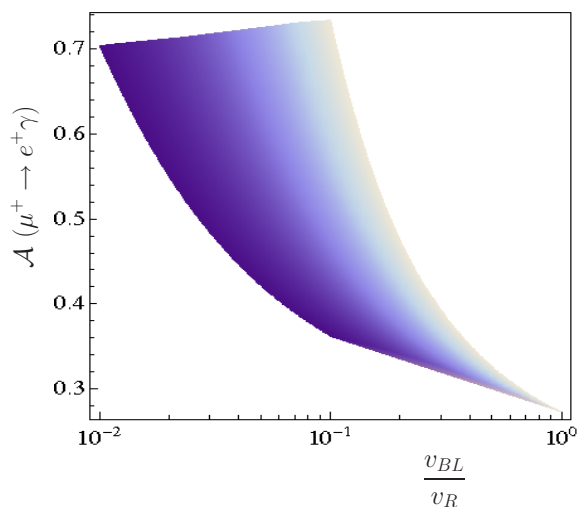


Figure 8. Positron polarization asymmetry $\mathcal{A}(\mu^+ \rightarrow e^+\gamma)$ as a function of the ratio v_{BL}/v_R . The seesaw scale M_S has been fixed to 10^{13} GeV, whereas v_{BL} and v_R take values in the ranges $v_{\text{BL}} \in [10^{14}, 10^{15}]$ GeV and $v_R \in [10^{15}, 10^{16}]$ GeV. Lighter colours indicate larger v_{BL} . The mSugra parameters have been taken as in the SPS3 benchmark point and neutrino oscillation data have been fitted with the Y_ν fit, assuming degenerate right-handed neutrinos.

more than the corresponding terms in the left-handed sector. The only possible exception to this general rule is, as discussed above, in the limit of very small m_0 and $v_{\text{BL}}/v_R \sim 1$.

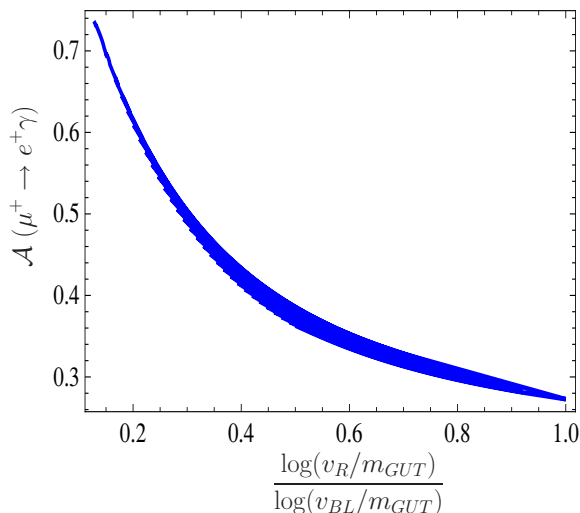


Figure 9. Positron polarization asymmetry $\mathcal{A}(\mu^+ \rightarrow e^+\gamma)$ as a function of $\log(v_R/m_{GUT})/\log(v_{BL}/m_{GUT})$. The parameters have been chosen as in figure 8.

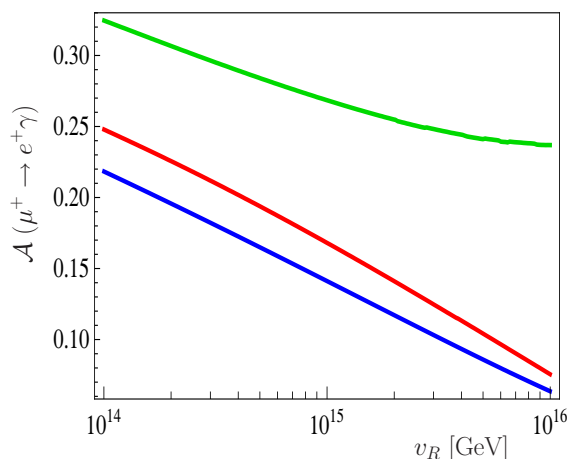


Figure 10. Positron polarization asymmetry $\mathcal{A}(\mu^+ \rightarrow e^+\gamma)$ as a function of v_R for three different mSUGRA benchmark points: SPS1a' (blue line), SPS3 (green line) and SPS5 (red line). In this figure a fixed value $v_{BL} = 10^{14}$ is taken. Neutrino oscillation data have been fitted with the f fit.

The determination of the ratio v_{BL}/v_R from figure 8 is shown to be very inaccurate. This is due to the fact that other parameters, most importantly m_{GUT} (which itself has an important dependence on the values of v_{BL} and v_R), have a strong impact on the results. Therefore, although it would be possible to constrain the high energy structure of the theory, a precise determination of the ratio v_{BL}/v_R will require additional input. Figure 9, on the other hand, shows that the polarization asymmetry $\mathcal{A}(\mu^+ \rightarrow e^+\gamma)$ is much better correlated with the quantity $\log(v_R/m_{GUT})/\log(v_{BL}/m_{GUT})$. This is as expected from equations (2.26) and (2.27) and confirms the validity of this approximation.

We close our discussion on the positron polarization asymmetry with some comments on the f fit. Since this type of fit leads to $\Delta m_L^2 \sim \Delta m_{e^c}^2 \sim 0$ in the $v_{BL} - v_R$ energy region, there is little dependence on these symmetry breaking scales. This is illustrated in figure 10, where the asymmetry \mathcal{A} is plotted as a function of v_R for three different mSUGRA benchmark points: SPS1a' (blue line), SPS3 (green line) and SPS5 (red line). One clearly sees that the dependence on v_R is quite weak compared to the Y_ν fit. In fact, the variations in this figure are mostly due to the changes in the low energy supersymmetric spectrum due to different v_R values. In the case of the f -fit one then typically finds $\mathcal{A} \in [0.0 - 0.3]$.

3.4 LFV at LHC/ILC

Lepton flavour violation might show up at collider experiments as well. Although the following discussion is focused on the LHC discovery potential for LFV signatures, let us emphasize that a future linear collider will be able to determine the relevant observables with much higher precision.

Figure 11 shows $Br(\tilde{\tau}_i \rightarrow \tilde{\chi}_1^0 e)$ and $Br(\tilde{\tau}_i \rightarrow \tilde{\chi}_1^0 \mu)$ as a function of the seesaw scale. The dashed lines correspond to $\tau_1 \simeq \tau_R$ and the solid ones to $\tau_2 \simeq \tau_L$. As in the case of $\mu \rightarrow e\gamma$, see figure 4, lower seesaw scales imply less flavour violating effects due to smaller Yukawa couplings. Moreover, figure 11 presents the same results for two different benchmark points, SPS1a' and SPS3. As already shown in figure 4, $\mu \rightarrow e\gamma$ is strongly dependent on the SUSY spectrum. For lighter supersymmetric particles, as in the benchmark point SPS1a', $\mu \rightarrow e\gamma$ is large, setting strong limits on the seesaw scale and thus on the possibility to observe LFV at colliders. In the case of heavier spectrums, as in SPS3, $\mu \rightarrow e\gamma$ is still the most stringent constraint, but larger values of the seesaw scale and thus LFV violating branching ratios become allowed. Whether decays such as $Br(\tilde{\tau}_i \rightarrow \tilde{\chi}_1^0 e)$ and $Br(\tilde{\tau}_i \rightarrow \tilde{\chi}_1^0 \mu)$ are observable at the LHC or not, thus depends very sensitively on the unknown m_0 , $M_{1/2}$ and M_S .

Furthermore, the right panel of figure 11 also shows that right staus can also have LFV decays with sizable rates. Of course, as emphasized already above, this is the main novelty of the LR model compared to pure seesaw models. This is direct consequence of parity restoration at high energies.

Moreover, as in our analysis of the positron polarization asymmetry, one expects to find that if the difference between v_R and v_{BL} is increased, the difference between the LFV entries in the L and R sectors gets increased as well. This property of the Y_ν fit is shown in figure 12, which shows branching ratios for the LFV decays of the staus as a function of v_{BL} for $v_R \in [10^{15}, 5 \cdot 10^{15}]$ GeV. As the figure shows, the theoretical expectation is confirmed numerically: the difference between $Br(\tilde{\tau}_L)$ and $Br(\tilde{\tau}_R)$ strongly depends on the difference between v_R and v_{BL} .

The question arises whether one can determine the ratio v_{BL}/v_R by measuring both $Br(\tilde{\tau}_L)$ and $Br(\tilde{\tau}_R)$ at colliders. Figure 13 attempts to answer this. Here the ratio $Br(\tilde{\tau}_R \rightarrow \tilde{\chi}_1^0 e)/Br(\tilde{\tau}_L \rightarrow \tilde{\chi}_1^0 e)$ is plotted as a function of v_{BL}/v_R . A measurement of both branching ratios would allow to constrain the ratio v_{BL}/v_R and increase our knowledge on the high energy regimes. For the sake of brevity we do not present here the analogous plots for other LFV slepton decays and/or other lepton final states, since they show very similar

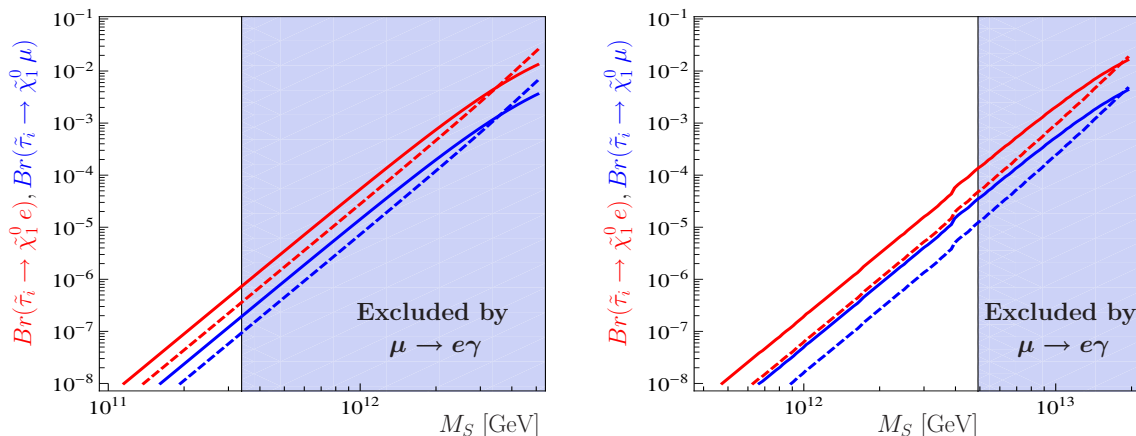


Figure 11. $Br(\tilde{\tau}_i \rightarrow \tilde{\chi}_1^0 e)$ and $Br(\tilde{\tau}_i \rightarrow \tilde{\chi}_1^0 \mu)$ as a function of the seesaw scale, defined as the mass of the lightest right-handed neutrino, for the parameter choice $v_{BL} = 10^{15}$ GeV and $v_R = 5 \cdot 10^{15}$ GeV. The dashed lines correspond to $\tau_1 \simeq \tau_R$ and the solid ones to $\tau_2 \simeq \tau_L$. To the left, the mSUGRA parameters have been taken as in the SPS1a' benchmark point, whereas to the right as in the SPS3 benchmark point. In both figures neutrino oscillation data have been fitted according to the f fit, with non-degenerate right-handed neutrinos. The blue shaded regions are excluded by $\mu \rightarrow e\gamma$.

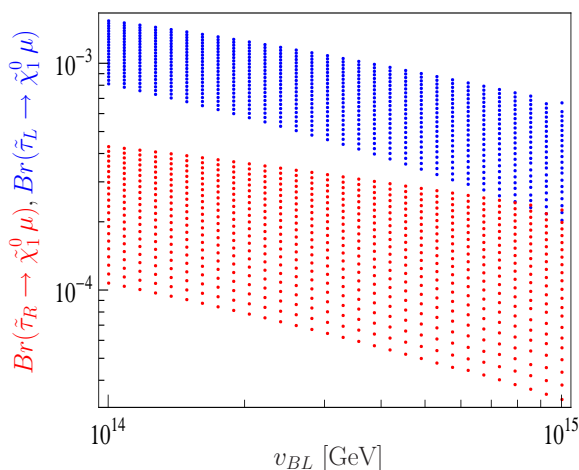


Figure 12. $Br(\tilde{\tau}_L \rightarrow \tilde{\chi}_1^0 \mu)$ and $Br(\tilde{\tau}_R \rightarrow \tilde{\chi}_1^0 \mu)$ as a function of v_{BL} for $M_S = 10^{13}$ GeV and $v_R \in [10^{15}, 5 \cdot 10^{15}]$ GeV. Red dots correspond to $\tau_1 \simeq \tau_R$, whereas the blue ones correspond to $\tau_2 \simeq \tau_L$. The mSUGRA parameters have been taken as in the SPS3 benchmark point and neutrino oscillation data have been fitted with the Y_ν fit, assuming degenerate right-handed neutrinos.

correlations with v_{BL}/v_R . For example, in principle, one could also use the ratio $Br(\tilde{\mu}_R \rightarrow \tilde{\chi}_1^0 \tau)/Br(\tilde{\mu}_L \rightarrow \tilde{\chi}_1^0 \tau)$ to determine the ratio between the two high scales.

However, as observed also in the polarization asymmetry for $\mu \rightarrow e\gamma$ there is an important dependence on other parameters of the model, especially the exact value of

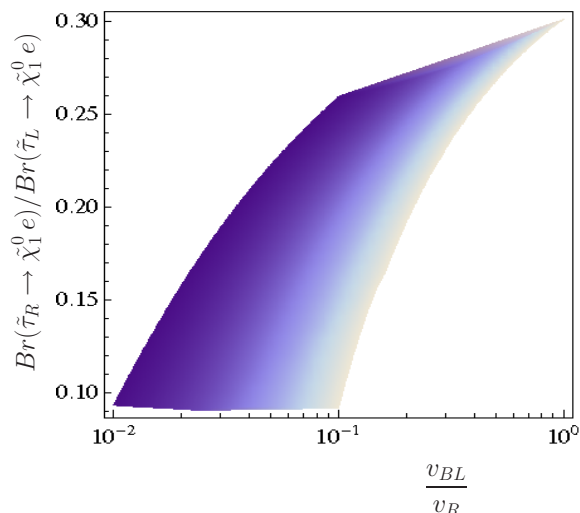


Figure 13. $Br(\tilde{\tau}_R \rightarrow \tilde{\chi}_1^0 e)/Br(\tilde{\tau}_L \rightarrow \tilde{\chi}_1^0 e)$ as a function of v_{BL}/v_R . The seesaw scale M_S has been fixed to 10^{13} GeV, whereas v_{BL} and v_R take values in the ranges $v_{BL} \in [10^{14}, 10^{15}]$ GeV and $v_R \in [10^{15}, 10^{16}]$ GeV. Lighter colours indicate larger v_{BL} . The rest of the parameters have been chosen as in figure 12.

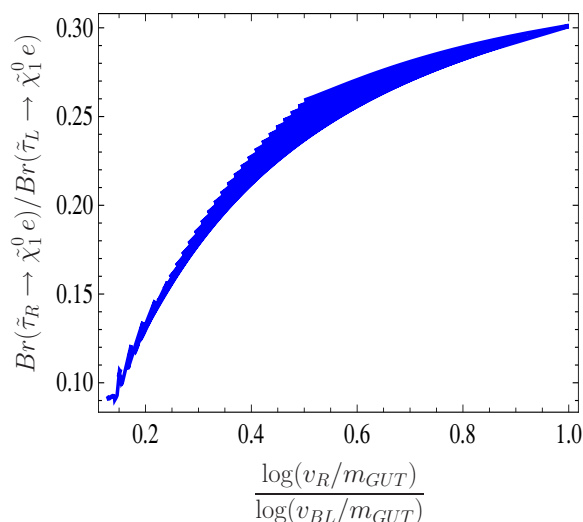


Figure 14. $Br(\tilde{\tau}_R \rightarrow \tilde{\chi}_1^0 e)/Br(\tilde{\tau}_L \rightarrow \tilde{\chi}_1^0 e)$ as a function of $\log(v_R/m_{GUT})/\log(v_{BL}/m_{GUT})$. The parameters have been chosen as in figure 13.

m_{GUT} . This implies a theoretical uncertainty in the determination of v_{BL}/v_R . Again, as for \mathcal{A} , a much better correlation with $\log(v_R/m_{GUT})/\log(v_{BL}/m_{GUT})$ is found, see figure 14.

In conclusion, to determine v_{BL} and v_R individually more *theoretical* input is needed, such as the GUT scale thresholds, which are needed to fix the value of m_{GUT} . Recall, that we did not specify the exact values of these thresholds in our numerical calculation. This leads to a “floating” value of m_{GUT} when v_R and v_{BL} are varied. Also more experimental data is needed to make more definite predictions. Especially SUSY mass

spectrum measurements, which may or may not be very precise at the LHC, depending on the SUSY point realized in nature, will be of great importance. Recall that, if in reach of a linear collider, slepton mass and branching ratio measurements can be highly precise.

So far only slepton decays have been discussed. This served to illustrate the most interesting signatures of the model, namely, lepton flavour violation in the right slepton sector. However, LHC searches for lepton flavour violation usually concentrate on the decay chain [83–85]

$$\tilde{\chi}_2^0 \rightarrow \tilde{l}^\pm l^\mp \rightarrow \tilde{\chi}_1^0 l^\pm l^\mp .$$

This well known signature has been widely studied due to the accurate information it can provide about the particle spectrum [86–90]. Note that in this decay one assumes usually that the $\tilde{\chi}_2^0$ themselves stem from the decay chain $\tilde{q}_L \rightarrow q\tilde{\chi}_2^0$. If the mass ordering $m_{\tilde{\chi}_2^0} > m_{\tilde{l}} > m_{\tilde{\chi}_1^0}$ is realized, the dilepton invariant mass [88, 91], defined as $m^2(l^+l^-) = (p_{l^+} + p_{l^-})^2$, has an edge structure with a prominent kinematical endpoint at

$$[m^2(l^+l^-)]_{\max} \equiv m_{ll}^2 = \frac{(m_{\tilde{\chi}_2^0}^2 - m_{\tilde{l}}^2)(m_{\tilde{l}}^2 - m_{\tilde{\chi}_1^0}^2)}{m_{\tilde{l}}^2} , \quad (3.8)$$

where the masses of the charged leptons have been neglected. The position of this edge can be measured with impressively high precision at the LHC [86–88], implying also an accurate determination of the intermediate slepton masses.

In fact, if two different sleptons $\tilde{l}_{1,2}$ have sufficiently high event rates for $\tilde{\chi}_2^0 \rightarrow \tilde{l}_{1,2}^\pm l_j^\mp \rightarrow \tilde{\chi}_1^0 l_i^\pm l_j^\mp$ and their masses allow these chains to be on-shell, two different dilepton edge distributions are expected [34, 92]. This presents a powerful tool to measure slepton mass splittings, which in turn allows to discriminate between the standard mSUGRA expectation, with usually negligible mass splittings for the first two generations, and extended models with additional sources of flavour violation.

The relation between the slepton mass splitting and the variation in the position of the kinematical is edge is found to be [34]

$$\frac{\Delta m_{ll}}{\bar{m}_{ll}} = \frac{\Delta m_{\tilde{l}}}{\bar{m}_{\tilde{l}}} \frac{m_{\tilde{\chi}_1^0}^2 m_{\tilde{\chi}_2^0}^2 - \bar{m}_{\tilde{l}}^4}{(\bar{m}_{\tilde{l}}^2 - m_{\tilde{\chi}_1^0}^2)(\bar{m}_{\tilde{l}}^2 - m_{\tilde{\chi}_2^0}^2)} . \quad (3.9)$$

Here $\Delta m_{ll}(i, j) = m_{l_i l_i} - m_{l_j l_j}$ is the difference between two edge positions, $\Delta m_{\tilde{l}} = m_{\tilde{l}_i} - m_{\tilde{l}_j}$ the difference between slepton masses and \bar{m}_{ll} and $\bar{m}_{\tilde{l}}$ average values of the corresponding quantities. Note that higher order contributions of $\frac{\Delta m_{\tilde{l}}}{\bar{m}_{\tilde{l}}}$ have been neglected in equation (3.9).

A number of studies about the dilepton mass distribution have been performed [86–88], concluding that the position of the edges can be measured at the LHC with an accuracy up to 10^{-3} . Moreover, as shown in reference [34], this can be generally translated into a similar precision for the relative $\tilde{e} - \tilde{\mu}$ mass splitting, with some regions of parameter space where values as small as 10^{-4} might be measurable. Since this mass splitting is usually negligible in a pure mSUGRA scenario, it is regarded as an interesting signature of either lepton flavour violation or non-universality in the soft terms. Furthermore, in the context

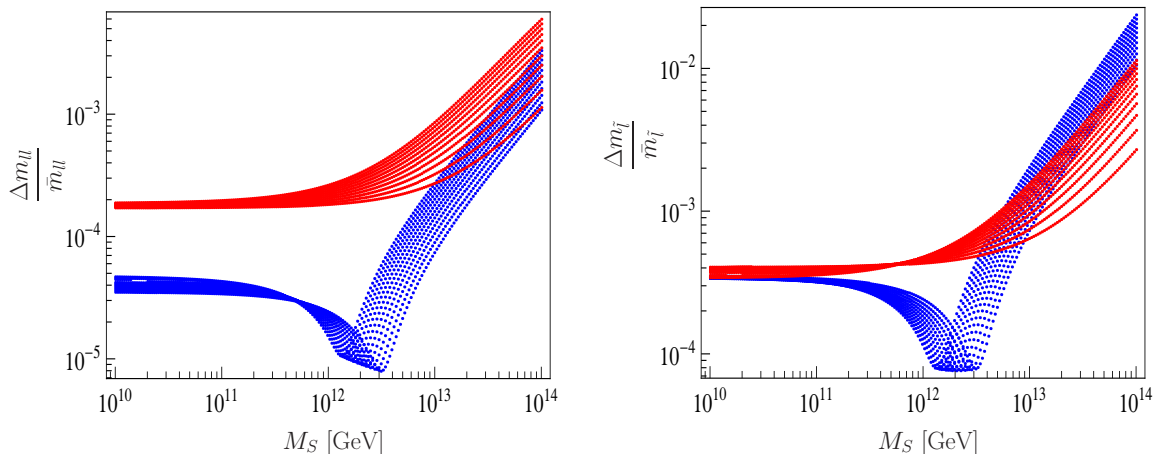


Figure 15. $\frac{\Delta m_{ll}}{m_{ll}}$ (left-hand side) and $\frac{\Delta m_{\bar{l}}}{m_{\bar{l}}}$ (right-hand side) as a function of the seesaw scale, defined as the mass of the lightest right-handed neutrino, for the parameter choice $v_{BL} = 10^{15}$ GeV and $v_R \in [10^{15}, 10^{16}]$ GeV. Blue dots correspond to the mass distribution generated by intermediate left sleptons whereas red dots correspond to the mass distribution generated by the right ones. The mSugra parameters have been taken as in the SPS3 benchmark point and neutrino oscillation data have been fitted according to the Y_{ν} fit, with degenerate right-handed neutrinos.

of this paper, it is important to emphasize that pure seesaw models can have this signature only in the left slepton sector [35].

Figure 15 shows our results for the observables $\frac{\Delta m_{ll}}{m_{ll}}$ and $\frac{\Delta m_{\bar{l}}}{m_{\bar{l}}}$ as a function of the seesaw scale. Large values for M_S lead to sizable deviations from the mSugra expectation, with a distinctive multi-edge structure in the dilepton mass distribution. Moreover, this effect is found in both left- and right- mediated decays. Observing this affect would clearly point towards a non-minimal seesaw model, such as the LR model we discuss.

As expected, these observables are correlated with other LFV signals [35, 93]. Figure 16 shows $Br(\mu \rightarrow e\gamma)$ as a function of $\left(\frac{\Delta m_{ll}}{m_{ll}}\right)_L$ (mass distribution with intermediate L sleptons) and $\left(\frac{\Delta m_{ll}}{m_{ll}}\right)_R$ (mass distribution with intermediate R sleptons). Again, the main novelty with respect to the usual seesaw implementations is the correlation in the right sector, not present in the minimal case [35].

Furthermore, the process $\tilde{\chi}_2^0 \rightarrow \tilde{\chi}_1^0 l_i^+ l_j^-$ might provide additional LFV signatures if the rate for decays with $l_i \neq l_j$ is sufficiently high. Reference [94] has investigated this possibility in great detail, performing a complete simulation of the CMS detector in the LHC for the decay $\tilde{\chi}_2^0 \rightarrow \tilde{\chi}_1^0 e\mu$. The result is given in terms of the quantity

$$K_{e\mu} = \frac{Br(\tilde{\chi}_2^0 \rightarrow \tilde{\chi}_1^0 e\mu)}{Br(\tilde{\chi}_2^0 \rightarrow \tilde{\chi}_1^0 ee) + Br(\tilde{\chi}_2^0 \rightarrow \tilde{\chi}_1^0 \mu\mu)}, \quad (3.10)$$

which parametrizes the amount of flavour violation in $\tilde{\chi}_2^0$ decays. The study, focused on the CMS test point LM1 ($m_0 = 60$ GeV, $M_{1/2} = 250$ GeV, $A_0 = 0$ GeV, $\tan\beta = 10$,

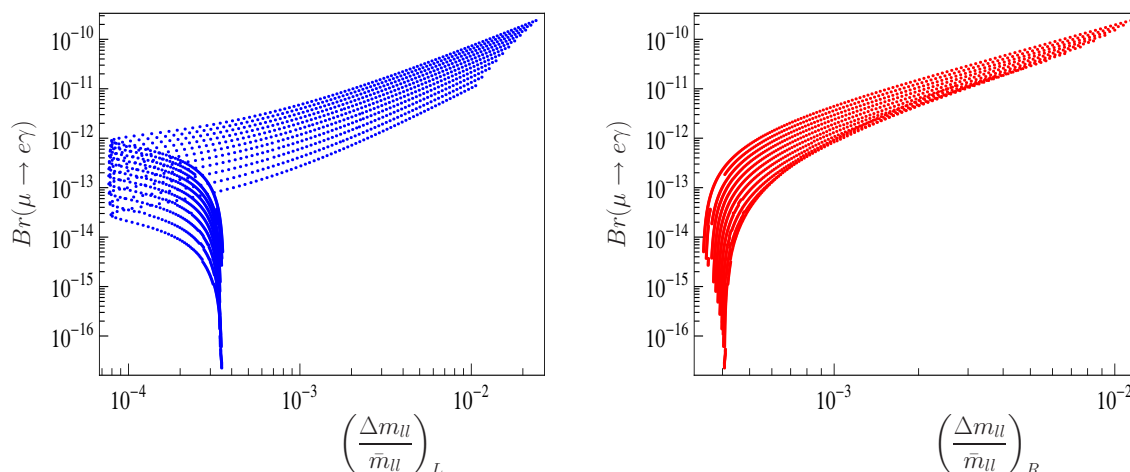


Figure 16. $Br(\mu \rightarrow e\gamma)$ as a function of $\left(\frac{\Delta m_u}{\bar{m}_u}\right)_L$ (left-hand side) and $\left(\frac{\Delta m_u}{\bar{m}_u}\right)_R$ (right-hand side). The parameters are chosen as in figure 15.

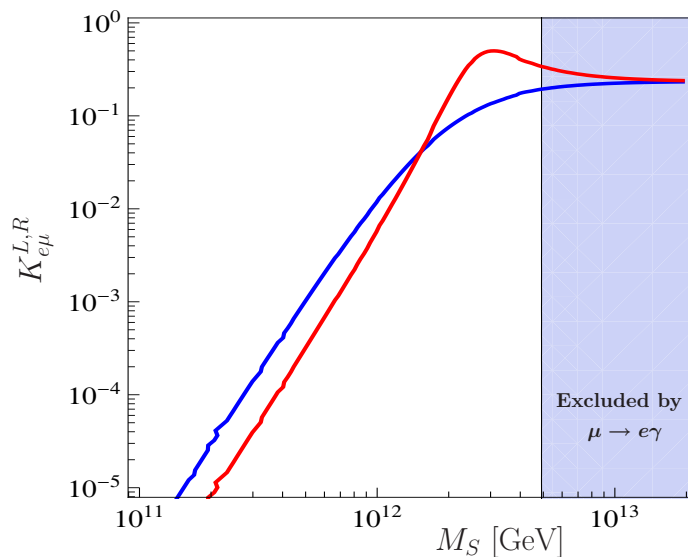


Figure 17. $K_{e\mu}$ as a function of the lightest right-handed neutrino mass, for the parameter choice $v_{BL} = 10^{15}$ GeV and $v_R = 5 \cdot 10^{15}$ GeV. The blue curve corresponds to contributions from intermediate L sleptons, whereas the red one corresponds to intermediate R sleptons. The mSugra parameters have been taken as in the SPS3 benchmark point, which satisfies $m(\tilde{\chi}_2^0) > m(\tilde{l}_i) > m(\tilde{\chi}_1^0)$, and thus the intermediate L and R sleptons can be produced on-shell. Neutrino oscillation data have been fitted according to the f fit, with non-degenerate right-handed neutrinos. The blue shaded region is excluded by $\mu \rightarrow e\gamma$.

$sign(\mu) = +$) [89], concludes that LFV can be discovered at the LHC at 5σ level with an integrated luminosity of $10 fb^{-1}$ if $K_{e\mu} \geq K_{e\mu}^{\min} = 0.04$.

Figure 17 shows our computation of $K_{e\mu}$ as a function of the lightest right-handed neutrino mass, for the parameter choice $v_{BL} = 10^{15}$ GeV and $v_R = 5 \cdot 10^{15}$ GeV. The results are shown splitting the contributions from intermediate left (blue) and right (red) sleptons. Although the selected mSugra parameters belong to the SPS3 point, and not to LM1 as in reference [94], a similar sensitivity for $K_{e\mu}^{\min}$ is expected.⁸ This is because the reduction in the cross-section due to the slightly heavier supersymmetric spectrum is possibly partially compensated by the corresponding reduction in the SM background and thus a limiting value $K_{e\mu}^{\min}$ of a similar order is expected. Moreover, [94] uses 10 fb^{-1} and with larger integrated luminosities even smaller $K_{e\mu}^{\min}$ should become accessible at the LHC.

The main result in figure 17 is that for large M_S values the rates for LFV $\tilde{\chi}_2^0$ decays are measurable for both left and right intermediate sleptons. In fact, for $M_S \gtrsim 10^{12}$ GeV the parameter $K_{e\mu}$ is above its minimum value for the 5σ discovery of $\tilde{\chi}_2^0 \rightarrow \tilde{\chi}_1^0 e\mu$. See references [94, 95] for more details on the LHC discovery potential in the search for LFV in this channel.

4 Conclusions

We have studied a supersymmetric left-right symmetric model. Our motivation for studying this setup was twofold. First, LR models are theoretically attractive, since they contain all the necessary ingredients to *generate* a seesaw mechanism, instead of adding it by hand as is so often done. And, second, in a setup where the SUSY LR is supplemented by flavour blind supersymmetry breaking boundary conditions, different from all pure seesaw setups, lepton flavour violation occurs in both, the left and the right slepton sectors.

We have calculated possible low-energy signals of this SUSY LR model, using full 2-loop RGEs for all parameters. We have found that low-energy lepton flavour violating decays, such as $\mu \rightarrow e\gamma$ are (a) expected to be larger than for the corresponding mSugra points in parameter space of seesaw type-I models and (b) the polarization asymmetry \mathcal{A} of the outgoing positron is found to differ significantly from the pure seesaw prediction of $\mathcal{A} = +1$ in large regions of parameter space. We have also discussed possible collider signatures of the SUSY LR model for LHC and a possible ILC. Mass splittings between smuons and selectrons and LFV violating slepton decays should occur in both the left and the right slepton sector, again different from the pure seesaw expectations.

We think therefore that the SUSY LR model is a good example of a “beyond” minimal, pure seesaw and offers many interesting novelties. For example, the impact of the intermediate scales on dark matter relic density and on certain mass combinations and the influence of the right-handed neutrino spectrum on low energy observables, are topics that certainly deserve further studies.

Acknowledgments

W.P. thanks IFIC/C.S.I.C. for hospitality. This work was supported by the Spanish MICINN under grants FPA2008-00319/FPA, by the MULTIDARK Consolider CSD2009-

⁸Moreover, the LM1 point, being very similar to SPS1a', is strongly constrained by $\mu \rightarrow e\gamma$.

00064, by Prometeo/2009/091, by the EU grant UNILHC PITN-GA-2009-237920 and FPA2008-04002-E/PORTU. A.V. thanks the Generalitat Valenciana for financial support and the people at CFTP in Lisbon for hospitality. The work of J. N. E. has been supported by *Fundação para a Ciência e a Tecnologia* through the fellowship SFRH/BD/29642/2006. J. N. E. and J. C. R. also acknowledge the financial support from *Fundação para a Ciência e a Tecnologia* grants CFTP-FCT UNIT 777 and CERN/FP/109305/2009. W.P. is partially supported by the German Ministry of Education and Research (BMBF) under contract 05HT6WWA and by the Alexander von Humboldt Foundation. F.S. has been supported by the DFG research training group GRK1147.

A RGEs

We present in the following appendices our results for the RGEs of the model above the $U(1)_{B-L}$ breaking scale. We will only show the β -functions for the gauge couplings and the anomalous dimensions of all chiral superfields. We briefly discuss in this section how these results were calculated. Furthermore, we show how they can be used to calculate the other β -functions of the models and give as example the 1-loop results for the soft SUSY breaking masses of the sleptons. The complete results are given online on this site

<http://theorie.physik.uni-wuerzburg.de/~fnst Staub/supplementary.html>

In addition, the corresponding model files for SARAH are also given on this web page.

A.1 Calculation of supersymmetric RGEs

For a general $N = 1$ supersymmetric gauge theory with superpotential

$$W(\phi) = \frac{1}{2}\mu^{ij}\phi_i\phi_j + \frac{1}{6}Y^{ijk}\phi_i\phi_j\phi_k \quad (\text{A.1})$$

the soft SUSY-breaking scalar terms are given by

$$V_{\text{soft}} = \left(\frac{1}{2}b^{ij}\phi_i\phi_j + \frac{1}{6}h^{ijk}\phi_i\phi_j\phi_k + \text{c.c.} \right) + (m^2)^i{}_j\phi_i\phi_j^* . \quad (\text{A.2})$$

The anomalous dimensions are given by [57]

$$\gamma_i^{(1)j} = \frac{1}{2}Y_{ipq}Y^{jpq} - 2\delta_i^j g^2 C_2(i) , \quad (\text{A.3})$$

$$\begin{aligned} \gamma_i^{(2)j} = & -\frac{1}{2}Y_{imn}Y^{npq}Y_{pqr}Y^{mrj} + g^2 Y_{ipq}Y^{jpq} [2C_2(p) - C_2(i)] \\ & + 2\delta_i^j g^4 [C_2(i)S(R) + 2C_2(i)^2 - 3C_2(G)C_2(i)] , \end{aligned} \quad (\text{A.4})$$

and the β -functions for the gauge couplings are given by

$$\beta_g^{(1)} = g^3 [S(R) - 3C_2(G)] , \quad (\text{A.5})$$

$$\beta_g^{(2)} = g^5 \{ -6[C_2(G)]^2 + 2C_2(G)S(R) + 4S(R)C_2(R) \} - g^3 Y^{ijk} Y_{ijk} C_2(k) / d(G) . \quad (\text{A.6})$$

Here, $C_2(i)$ is the quadratic Casimir for a specific superfield and $C_2(R), C_2(G)$ are the quadratic Casimirs for the matter and adjoint representations, respectively. $d(G)$ is the dimension of the adjoint representation.

The β -functions for the superpotential parameters can be obtained by using superfield technique. The obtained expressions are [96, 97].

$$\beta_Y^{ijk} = Y^{p(ij} \gamma_p^{k)}, \quad (\text{A.7})$$

$$\beta_\mu^{ij} = \mu^{p(i} \gamma_p^{j)}. \quad (\text{A.8})$$

The (..) in the superscripts denote symmetrization. Most of the β -functions of the models can be derived from these results using the procedure given in [98] based on the spurion formalism [99]. In the following, we briefly summarize the basic ideas of this calculation for completeness.

The exact results for the soft β -functions are given by [98]:

$$\beta_M = 2\mathcal{O} \left[\frac{\beta_g}{g} \right], \quad (\text{A.9})$$

$$\begin{aligned} \beta_h^{ijk} &= h^{l(jk} \gamma_l^i) - 2Y^{l(jk} \gamma_1^i)_l, \\ \beta_b^{ij} &= b^{l(i} \gamma_l^{j)} - 2\mu^{l(i} \gamma_1^j)_l, \\ (\beta_{m^2})^i_j &= \Delta \gamma^i_j. \end{aligned} \quad (\text{A.10})$$

where we defined

$$\mathcal{O} = Mg^2 \frac{\partial}{\partial g^2} - h^{lmn} \frac{\partial}{\partial Y^{lmn}}, \quad (\text{A.11})$$

$$(\gamma_1)^i_j = \mathcal{O} \gamma^i_j, \quad (\text{A.12})$$

$$\Delta = 2\mathcal{O}\mathcal{O}^* + 2MM^* g^2 \frac{\partial}{\partial g^2} + \left[\tilde{Y}^{lmn} \frac{\partial}{\partial Y^{lmn}} + \text{c.c.} \right] + X \frac{\partial}{\partial g}. \quad (\text{A.13})$$

Here, M is the gaugino mass and $\tilde{Y}^{ijk} = (m^2)_i Y^{jkl} + (m^2)_j Y^{ikl} + (m^2)_k Y^{ijl}$. Eqs. (A.9)–(A.10) hold in a class of renormalization schemes that includes the DRED'-one [100]. We take the known contributions of X from [101]:

$$X^{\text{DRED}'(1)} = -2g^3 S, \quad (\text{A.14})$$

$$X^{\text{DRED}'(2)} = (2r)^{-1} g^3 \text{tr}[WC_2(R)] - 4g^5 C_2(G)S - 2g^5 C_2(G)QMM^*, \quad (\text{A.15})$$

where

$$S = r^{-1} \text{tr}[m^2 C_2(R)] - MM^* C_2(G), \quad (\text{A.16})$$

$$\begin{aligned} W^j_i &= \frac{1}{2} Y_{ipq} Y^{pqn} (m^2)^j_n + \frac{1}{2} Y^{jpa} Y_{pqn} (m^2)^n_i + 2Y_{ipq} Y^{jpr} (m^2)^q_r \\ &\quad + h_{ipq} h^{jpa} - 8g^2 MM^* C_2(R)^j_i. \end{aligned} \quad (\text{A.17})$$

With $Q = T(R) - 3C_2(G)$, and $T(R) = \text{tr}[C_2(R)]$, r being the number of group generators.

A.2 From GUT scale to $SU(2)_R$ breaking scale

In the following sections we will use the definitions

$$Y_{Q_k}^{ij} = Y_Q^{ijk}, \quad Y_{L_k}^{ij} = Y_L^{ijk} \quad (\text{A.18})$$

and in the same way $T_{Q_k}^{ij}$ and $T_{L_k}^{ij}$. We will also assume summation of repeated indices.

A.2.1 Anomalous dimensions

$$\gamma_{\hat{Q}}^{(1)} = 2Y_{Q_k}^* Y_{Q_k}^T - \frac{1}{12} (18g_2^2 + 32g_3^2 + g_{\text{BL}}^2) \mathbf{1} \quad (\text{A.19})$$

$$\begin{aligned} \gamma_{\hat{Q}}^{(2)} = & + \frac{1}{144} \left(-128g_3^4 + 2052g_2^4 + 289g_{\text{BL}}^4 + 36g_2^2 (32g_3^2 + g_{\text{BL}}^2) + 64g_3^2 g_{\text{BL}}^2 \right) \mathbf{1} \\ & + Y_{Q_m}^* \left(6g_2^2 \delta_{mn} + \frac{27}{4} \text{Tr}(\alpha\alpha^*) \delta_{mn} - 2\text{Tr}(Y_{L_n}^* Y_{L_m}^T) - 6\text{Tr}(Y_{Q_n}^* Y_{Q_m}^T) \right) Y_{Q_n}^T \\ & - 32Y_{Q_m}^* Y_{Q_n}^\dagger Y_{Q_n} Y_{Q_m}^T \end{aligned} \quad (\text{A.20})$$

$$\gamma_{\hat{Q}^c}^{(1)} = 2Y_{Q_k}^\dagger Y_{Q_k} - \frac{1}{12} (18g_2^2 + 32g_3^2 + g_{\text{BL}}^2) \mathbf{1} \quad (\text{A.21})$$

$$\begin{aligned} \gamma_{\hat{Q}^c}^{(2)} = & + \frac{1}{144} \left(-128g_3^4 + 2052g_2^4 + 289g_{\text{BL}}^4 + 36g_2^2 (32g_3^2 + g_{\text{BL}}^2) + 64g_3^2 g_{\text{BL}}^2 \right) \mathbf{1} \\ & + Y_{Q_m}^\dagger \left(6g_2^2 \delta_{mn} + \frac{27}{4} \text{Tr}(\alpha\alpha^*) \delta_{mn} - 2\text{Tr}(Y_{L_n}^* Y_{L_m}^T) - 6\text{Tr}(Y_{Q_n}^* Y_{Q_m}^T) \right) Y_{Q_n} \\ & - 32Y_{Q_m}^\dagger Y_{Q_n} Y_{Q_m}^T Y_{Q_n}^* \end{aligned} \quad (\text{A.22})$$

$$\gamma_{\hat{L}}^{(1)} = 2(3f^\dagger f + Y_{L_k}^* Y_{L_k}^T) - \frac{3}{4} (2g_2^2 + g_{\text{BL}}^2) \mathbf{1} \quad (\text{A.23})$$

$$\begin{aligned} \gamma_{\hat{L}}^{(2)} = & \frac{3}{16} (12g_2^2 g_{\text{BL}}^2 + 76g_2^4 + 99g_{\text{BL}}^4) \mathbf{1} + 3f^\dagger f \left(-3|a|^2 - 4\text{Tr}(ff^\dagger) + 6g_{\text{BL}}^2 + 8g_2^2 \right) \\ & + Y_{L_m}^* \left(6g_2^2 \delta_{mn} + \frac{27}{4} \text{Tr}(\alpha\alpha^*) \delta_{mn} - 2\text{Tr}(Y_{L_n}^* Y_{L_m}^T) - 6\text{Tr}(Y_{Q_n}^* Y_{Q_m}^T) \right. \\ & \quad \left. - 11f^\dagger f \delta_{mn} \right) Y_{L_n}^T - 4Y_{L_m}^* Y_{L_n}^\dagger Y_{L_n} Y_{L_m}^T - 2f^\dagger (17ff^\dagger + 3Y_{L_k} Y_{L_k}^\dagger) f \\ & - 6f^\dagger Y_{L_k} f Y_{L_k}^* \end{aligned} \quad (\text{A.24})$$

$$\gamma_{\hat{L}^c}^{(1)} = 2(3ff^\dagger + Y_{L_k}^\dagger Y_{L_k}) - \frac{3}{4} (2g_2^2 + g_{\text{BL}}^2) \mathbf{1} \quad (\text{A.25})$$

$$\begin{aligned} \gamma_{\hat{L}^c}^{(2)} = & \frac{3}{16} (12g_2^2 g_{\text{BL}}^2 + 76g_2^4 + 99g_{\text{BL}}^4) \mathbf{1} + 3ff^\dagger \left(-3|a|^2 - 4\text{Tr}(ff^\dagger) + 6g_{\text{BL}}^2 + 8g_2^2 \right) \\ & + Y_{L_m}^\dagger \left(6g_2^2 \delta_{mn} + \frac{27}{4} \text{Tr}(\alpha\alpha^*) \delta_{mn} - 2\text{Tr}(Y_{L_n}^* Y_{L_m}^T) - 6\text{Tr}(Y_{Q_n}^* Y_{Q_m}^T) \right. \\ & \quad \left. - 11ff^\dagger \delta_{mn} \right) Y_{L_n} - 4Y_{L_m}^\dagger Y_{L_n} Y_{L_m}^T Y_{L_n}^* - 2f \left(17f^\dagger f + 3Y_{L_k}^T Y_{L_k}^* \right) f^\dagger \\ & - 6Y_{L_k}^\dagger Y_{L_k} f f^\dagger \end{aligned} \quad (\text{A.26})$$

$$(\gamma_{\hat{\Phi}}^{(1)})_{ij} = -3g_2^2 \mathbf{1} - \frac{3}{2} (\alpha\alpha^* + \alpha^* \alpha) + \delta_{im} \delta_{jn} \left(3\text{Tr}(Y_{Q_m}^* Y_{Q_n}^T) + \text{Tr}(Y_{L_m}^* Y_{L_n}^T) \right) \quad (\text{A.27})$$

$$\begin{aligned} (\gamma_{\hat{\Phi}}^{(2)})_{ij} = & 33g_2^4 \mathbf{1} - 9 \left(2(\alpha\alpha\alpha^* \alpha^* + \alpha^* \alpha^* \alpha\alpha) + 3(\alpha\alpha^* \alpha\alpha^* + \alpha^* \alpha\alpha^* \alpha) \right) \\ & - 24(\alpha\alpha^* + \alpha^* \alpha) (2g_2^2 + 2\text{Tr}(\alpha\alpha^*) - |a|^2) \end{aligned}$$

$$\begin{aligned}
 & -\frac{3}{2}(\alpha_{jm}\alpha_{in}^* + \alpha_{jm}^*\alpha_{in})\left(3\text{Tr}(Y_{Q_m}^* Y_{Q_n}^T) + \text{Tr}(Y_{L_m}^* Y_{L_n}^T)\right) \\
 & -\frac{1}{2}\delta_{im}\delta_{in}\left(-3g_{\text{BL}}^2\text{Tr}(Y_{L_m}^* Y_{L_n}^T) - (32g_3^2 + g_{\text{BL}}^2)\text{Tr}(Y_{Q_m}^* Y_{Q_n}^T)\right) \\
 & + 2\left(5\text{Tr}(f f^\dagger Y_{L_n} Y_{L_m}^\dagger) + \text{Tr}(f Y_{L_n}^* Y_{L_m}^T f^\dagger) + 6\text{Tr}(f Y_{L_m}^* Y_{L_n}^T f^\dagger)\right) \\
 & + 4\left(2\text{Tr}(Y_{L_m}^\dagger Y_{L_n} Y_{L_n}^T Y_{L_m}^*) + \text{Tr}(Y_{L_m}^\dagger Y_{L_m} Y_{L_n}^T Y_{L_m}^*) + \text{Tr}(Y_{L_m}^\dagger Y_{L_n} Y_{L_m}^T Y_{L_n}^*)\right) \\
 & + 12\left(2\text{Tr}(Y_{Q_m}^\dagger Y_{Q_n} Y_{Q_n}^T Y_{Q_m}^*) + \text{Tr}(Y_{Q_m}^\dagger Y_{Q_m} Y_{Q_n}^T Y_{Q_m}^*)\right) \\
 & + \text{Tr}(Y_{Q_m}^\dagger Y_{Q_n} Y_{Q_m}^T Y_{Q_n}^*) \Big) \Big) \tag{A.28}
 \end{aligned}$$

$$\gamma_{\hat{\Delta}}^{(1)} = 2\text{Tr}(f f^\dagger) - 3g_{\text{BL}}^2 - 4g_2^2 + \frac{3}{2}|a|^2 \tag{A.29}$$

$$\begin{aligned}
 \gamma_{\hat{\Delta}}^{(2)} &= 48g_2^4 + 24g_2^2 g_{\text{BL}}^2 + 81g_{\text{BL}}^4 \\
 &+ \frac{3}{2}|a|^2\left(4g_2^2 + \text{Tr}(\alpha\alpha^*) - \frac{7}{2}|a|^2\right) - (2g_2^2 + 3g_{\text{BL}}^2)\text{Tr}(f f^\dagger) \\
 &- 24\text{Tr}(f f^\dagger f f^\dagger) - 6\text{Tr}(f f^\dagger Y_{L_k} Y_{L_k}^\dagger) - 2\text{Tr}(f Y_{L_k}^* Y_{L_k}^T f^\dagger) \tag{A.30}
 \end{aligned}$$

$$\gamma_{\hat{\Delta}}^{(1)} = -3g_{\text{BL}}^2 - 4g_2^2 + \frac{3}{2}|a|^2 \tag{A.31}$$

$$\begin{aligned}
 \gamma_{\hat{\Delta}}^{(2)} &= \frac{3}{4}\left(4\left(16g_2^4 + 27g_{\text{BL}}^4 + 8g_2^2 g_{\text{BL}}^2\right)\right. \\
 &\left. + |a|^2\left(2\text{Tr}(\alpha\alpha^*) - 3\text{Tr}(f f^\dagger) - 7|a|^2 + 8g_2^2\right)\right) \tag{A.32}
 \end{aligned}$$

$$\gamma_{\hat{\Delta}^c}^{(1)} = 2\text{Tr}(f f^\dagger) - 3g_{\text{BL}}^2 - 4g_2^2 + \frac{3}{2}|a|^2 \tag{A.33}$$

$$\begin{aligned}
 \gamma_{\hat{\Delta}^c}^{(2)} &= 48g_2^4 + 24g_2^2 g_{\text{BL}}^2 + 81g_{\text{BL}}^4 \\
 &+ \frac{3}{2}|a|^2\left(4g_2^2 + \text{Tr}(\alpha\alpha^*) - \frac{7}{2}|a|^2\right) - (2g_2^2 + 3g_{\text{BL}}^2)\text{Tr}(f f^\dagger) \\
 &- 24\text{Tr}(f f^\dagger f f^\dagger) - 8\text{Tr}(f Y_{L_k}^T Y_{L_k}^* f^\dagger) \tag{A.34}
 \end{aligned}$$

$$\gamma_{\hat{\Delta}^c}^{(1)} = -3g_{\text{BL}}^2 - 4g_2^2 + \frac{3}{2}|a|^2 \tag{A.35}$$

$$\begin{aligned}
 \gamma_{\hat{\Delta}^c}^{(2)} &= \frac{3}{4}\left(4\left(16g_2^4 + 27g_{\text{BL}}^4 + 8g_2^2 g_{\text{BL}}^2\right)\right. \\
 &\left. + |a|^2\left(2\text{Tr}(\alpha\alpha^*) - 3\text{Tr}(f f^\dagger) - 7|a|^2 + 8g_2^2\right)\right) \tag{A.36}
 \end{aligned}$$

$$\gamma_{\hat{\Omega}}^{(1)} = 2|a|^2 - 4g_2^2 \tag{A.37}$$

$$\gamma_{\hat{\Omega}}^{(2)} = 3\text{Tr}(\alpha(\alpha\alpha^* - \alpha^*\alpha)\alpha^*) + 48g_2^4 + |a|^2\left(12g_{\text{BL}}^2 - 3\text{Tr}(f f^\dagger) - 6|a|^2 + 8g_2^2\right) \tag{A.38}$$

$$\gamma_{\hat{\Omega}^c}^{(1)} = 2|a|^2 - 4g_2^2 \tag{A.39}$$

$$\gamma_{\hat{\Omega}^c}^{(2)} = 3\text{Tr}(\alpha(\alpha\alpha^* - \alpha^*\alpha)\alpha^*) + 48g_2^4 + |a|^2\left(12g_{\text{BL}}^2 - 3\text{Tr}(f f^\dagger) - 6|a|^2 + 8g_2^2\right) \tag{A.40}$$

Note that the previous formulas are totally general and can be applied with any number of bidoublets. Nevertheless, if two bidoublets are considered $\alpha\alpha^* = \alpha^*\alpha$ and further simplifications are possible.

A.2.2 Beta functions for soft breaking masses of sleptons

Using the procedure explained in section A.1, we can calculate the soft breaking masses for the sleptons. The results are

$$\begin{aligned}
16\pi^2 \frac{d}{dt} m_L^2 &= 6ff^\dagger m_L^2 + 12fm_L^2 f^\dagger + 6m_L^2 f f^\dagger + 12m_\Delta^2 f f^\dagger \\
&\quad + 2Y_{L_k} Y_{L_k}^\dagger m_L^2 + 2m_L^2 Y_{L_k} Y_{L_k}^\dagger + 4Y_{L_k} m_{L_c}^2 Y_{L_k}^\dagger \\
&\quad + 4(m_\Phi^2)_{mn} Y_L^{(m)} Y_L^{(n)\dagger} + 12T_f T_f^\dagger + 4T_{L_k} T_{L_k}^\dagger \\
&\quad - (3g_{\text{BL}}^2 |M_1|^2 + 6g_2^2 |M_2|^2 + \frac{3}{2} g_{\text{BL}}^2 S_1) \mathbf{1}
\end{aligned} \tag{A.41}$$

$$\begin{aligned}
16\pi^2 \frac{d}{dt} m_{L_c}^2 &= 6f^\dagger f m_{L_c}^2 + 12f^\dagger m_{L_c}^2 f + 6m_{L_c}^2 f^\dagger f + 12m_{\Delta_c}^2 f^\dagger f \\
&\quad + 2Y_{L_k}^\dagger Y_{L_k} m_{L_c}^2 + 2m_{L_c}^2 Y_{L_k}^\dagger Y_{L_k} + 4Y_{L_k}^\dagger m_L^2 Y_{L_k} \\
&\quad + 4(m_\Phi^2)_{mn} Y_L^{(m)\dagger} Y_L^{(n)} + 12T_f^\dagger T_f + 4T_{L_k}^\dagger T_{L_k} \\
&\quad - (3g_{\text{BL}}^2 |M_1|^2 + 6g_2^2 |M_2|^2 - \frac{3}{2} g_{\text{BL}}^2 S_1) \mathbf{1}
\end{aligned} \tag{A.42}$$

where

$$\begin{aligned}
S_1 &= 3(m_\Delta^2 - m_{\bar{\Delta}}^2 - m_{\Delta_c}^2 + m_{\bar{\Delta}_c}^2) \\
&\quad + \sum_{m,n} [(m_Q^2)_{mn} - (m_{Q_c}^2)_{mn} - (m_L^2)_{mn} + (m_{L_c}^2)_{mn}]
\end{aligned} \tag{A.43}$$

A.2.3 Beta functions for gauge couplings

$$\beta_{g_{\text{BL}}}^{(1)} = 24g_{\text{BL}}^3 \tag{A.44}$$

$$\begin{aligned}
\beta_{g_{\text{BL}}}^{(2)} &= \frac{1}{2} g_{\text{BL}}^3 \left(-192|a|^2 - 93\text{Tr}(ff^\dagger) + 2(115g_{\text{BL}}^2 + 162g_2^2 \right. \\
&\quad \left. - 2\text{Tr}(Y_{Q_k}^* Y_{Q_k}^T) - 6\text{Tr}(Y_{L_k}^* Y_{L_k}^T) + 8g_3^2 \right)
\end{aligned} \tag{A.45}$$

$$\beta_{g_2}^{(1)} = 8g_2^3 \tag{A.46}$$

$$\begin{aligned}
\beta_{g_2}^{(2)} &= \frac{1}{6} g_2^3 \left(660g_2^2 + 144g_3^2 + 162g_{\text{BL}}^2 - 192|a|^2 + 108\text{Tr}(\alpha\alpha^*) - 73\text{Tr}(ff^\dagger) \right. \\
&\quad \left. - 24\text{Tr}(Y_{L_k}^* Y_{L_k}^T) - 72\text{Tr}(Y_{Q_k}^* Y_{Q_k}^T) \right)
\end{aligned} \tag{A.47}$$

$$\beta_{g_3}^{(1)} = -3g_3^3 \tag{A.48}$$

$$\beta_{g_3}^{(2)} = g_3^3 \left(14g_3^2 + 18g_2^2 - 8\text{Tr}(Y_{Q_k}^* Y_{Q_k}^T) + g_{\text{BL}}^2 \right) \tag{A.49}$$

A.3 From $SU(2)_R$ breaking scale to $U(1)_{B-L}$ breaking scale

A.3.1 Anomalous dimensions

$$\gamma_Q^{(1)} = -\frac{1}{12} \left(18g_L^2 + 32g_3^2 + g_{\text{BL}}^2 \right) \mathbf{1} + Y_d^* Y_d^T + Y_u^* Y_u^T \tag{A.50}$$

$$\gamma_Q^{(2)} = +\frac{1}{144} \left(109g_{\text{BL}}^4 - 128g_3^4 + 36g_{\text{BL}}^2 g_L^2 + 64g_3^2 (18g_L^2 + g_{\text{BL}}^2) + 972g_L^4 \right) \mathbf{1}$$

$$\begin{aligned}
& -2\left(Y_d^* Y_d^T Y_d^* Y_d^T + Y_u^* Y_u^T Y_u^* Y_u^T\right) \\
& + Y_d^* Y_d^T \left(-3\text{Tr}\left(Y_d Y_d^\dagger\right) - |b_c|^2 - \frac{3}{2}|b|^2 - \text{Tr}\left(Y_e Y_e^\dagger\right) + g_R^2\right) \\
& + Y_u^* Y_u^T \left(-3\text{Tr}\left(Y_u Y_u^\dagger\right) - |b_c|^2 - \frac{3}{2}|b|^2 - \text{Tr}\left(Y_\nu Y_\nu^\dagger\right) + g_R^2\right)
\end{aligned} \tag{A.51}$$

$$\gamma_{\hat{d}c}^{(1)} = 2Y_d^\dagger Y_d - \frac{1}{12}\left(32g_3^2 + 6g_R^2 + g_{\text{BL}}^2\right)\mathbf{1} \tag{A.52}$$

$$\begin{aligned}
\gamma_{\hat{d}c}^{(2)} = & -\frac{1}{144}\left(-109g_{\text{BL}}^4 + 128g_3^4 - 12g_{\text{BL}}^2 g_R^2 - 64g_3^2\left(6g_R^2 + g_{\text{BL}}^2\right) - 684g_R^4\right)\mathbf{1} \\
& -2\left(Y_d^\dagger Y_d Y_d^\dagger Y_d + Y_d^\dagger Y_u Y_u^\dagger Y_d\right) \\
& -Y_d^\dagger Y_d\left(2|b_c|^2 + 2\text{Tr}\left(Y_e Y_e^\dagger\right) + 3|b|^2 - 6g_L^2 + 6\text{Tr}\left(Y_d Y_d^\dagger\right)\right)
\end{aligned} \tag{A.53}$$

$$\gamma_{\hat{u}c}^{(1)} = 2Y_u^\dagger Y_u - \frac{1}{12}\left(32g_3^2 + 6g_R^2 + g_{\text{BL}}^2\right)\mathbf{1} \tag{A.54}$$

$$\begin{aligned}
\gamma_{\hat{u}c}^{(2)} = & -\frac{1}{144}\left(-109g_{\text{BL}}^4 + 128g_3^4 - 12g_{\text{BL}}^2 g_R^2 - 64g_3^2\left(6g_R^2 + g_{\text{BL}}^2\right) - 684g_R^4\right)\mathbf{1} \\
& -2\left(Y_u^\dagger Y_d Y_d^\dagger Y_u + Y_u^\dagger Y_u Y_u^\dagger Y_u\right) \\
& -Y_u^\dagger Y_u\left(2|b_c|^2 + 2\text{Tr}\left(Y_\nu Y_\nu^\dagger\right) + 3|b|^2 - 6g_L^2 + 6\text{Tr}\left(Y_u Y_u^\dagger\right)\right)
\end{aligned} \tag{A.55}$$

$$\gamma_{\hat{L}}^{(1)} = -\frac{3}{4}\left(2g_L^2 + g_{\text{BL}}^2\right)\mathbf{1} + Y_e^* Y_e^T + Y_\nu^* Y_\nu^T \tag{A.56}$$

$$\begin{aligned}
\gamma_{\hat{L}}^{(2)} = & +\frac{9}{16}\left(12g_L^4 + 13g_{\text{BL}}^4 + 4g_{\text{BL}}^2 g_L^2\right)\mathbf{1} - 2\left(Y_e^* Y_e^T Y_e^* Y_e^T + Y_\nu^* Y_\nu^T Y_\nu^* Y_\nu^T\right) \\
& -Y_\nu^* F_c Y_\nu^T \\
& + Y_e^* Y_e^T \left(-3\text{Tr}\left(Y_d Y_d^\dagger\right) - |b_c|^2 - \frac{3}{2}|b|^2 - \text{Tr}\left(Y_e Y_e^\dagger\right) + g_R^2\right) \\
& + Y_\nu^* Y_\nu^T \left(-3\text{Tr}\left(Y_u Y_u^\dagger\right) - |b_c|^2 - \frac{3}{2}|b|^2 - \text{Tr}\left(Y_\nu Y_\nu^\dagger\right) + g_R^2\right)
\end{aligned} \tag{A.57}$$

$$\gamma_{\hat{e}c}^{(1)} = 2Y_e^\dagger Y_e - \frac{1}{4}\left(2g_R^2 + 3g_{\text{BL}}^2\right)\mathbf{1} \tag{A.58}$$

$$\begin{aligned}
\gamma_{\hat{e}c}^{(2)} = & +\frac{1}{16}\left(117g_{\text{BL}}^4 + 12g_{\text{BL}}^2 g_R^2 + 76g_R^4\right)\mathbf{1} - 2\left(Y_e^\dagger Y_e Y_e^\dagger Y_e + Y_e^\dagger Y_\nu Y_\nu^\dagger Y_e\right) \\
& -Y_e^\dagger Y_e\left(2|b_c|^2 + 2\text{Tr}\left(Y_e Y_e^\dagger\right) + 3|b|^2 - 6g_L^2 + 6\text{Tr}\left(Y_d Y_d^\dagger\right)\right)
\end{aligned} \tag{A.59}$$

$$\gamma_{\hat{\nu}c}^{(1)} = 2Y_\nu^\dagger Y_\nu - \frac{1}{4}\left(2g_R^2 + 3g_{\text{BL}}^2\right)\mathbf{1} + F_c^* \tag{A.60}$$

$$\begin{aligned}
\gamma_{\hat{\nu}c}^{(2)} = & \frac{1}{16}\left(117g_{\text{BL}}^4 + 12g_{\text{BL}}^2 g_R^2 + 76g_R^4\right)\mathbf{1} - (f_c^{1\dagger} + f_c^{1*})F_c(f_c^1 + f_c^{1T}) \\
& -2Y_\nu^\dagger\left(Y_e Y_e^\dagger + Y_\nu Y_\nu^\dagger\right)Y_\nu - 2(f_c^{1\dagger} + f_c^{1*})Y_\nu^T Y_\nu^*(f_c^1 + f_c^{1T}) \\
& -Y_\nu^\dagger Y_\nu\left(2\left(-3g_L^2 + 3\text{Tr}\left(Y_u Y_u^\dagger\right) + |b_c|^2 + \text{Tr}\left(Y_\nu Y_\nu^\dagger\right)\right) + 3|b|^2\right) \\
& + F_c^*\left(2g_R^2 + 3g_{\text{BL}}^2 - |a_c^1|^2 - \text{Tr}\left(f_c^1 f_c^{1\dagger}\right) - \text{Tr}\left(f_c^{1\dagger} f_c^{1T}\right)\right)
\end{aligned} \tag{A.61}$$

$$\gamma_{\hat{H}_d}^{(1)} = 3\text{Tr}\left(Y_d Y_d^\dagger\right) - \frac{1}{2}g_R^2 + \frac{3}{2}|b|^2 - \frac{3}{2}g_L^2 + |b_c|^2 + \text{Tr}\left(Y_e Y_e^\dagger\right) \tag{A.62}$$

$$\gamma_{\hat{H}_d}^{(2)} = \frac{1}{4}\left(27g_L^4 + 6g_L^2 g_R^2 + 19g_R^4 + 2\left(32g_3^2 + g_{\text{BL}}^2\right)\text{Tr}\left(Y_d Y_d^\dagger\right) + 6g_{\text{BL}}^2 \text{Tr}\left(Y_e Y_e^\dagger\right)\right)$$

$$\begin{aligned}
 & + |b|^2 \left(-18\text{Tr}(Y_u Y_u^\dagger) - 15|b|^2 - 19|b_c|^2 + 24g_L^2 - 6\text{Tr}(Y_\nu Y_\nu^\dagger) \right) \\
 & - 4|b_c|^2 \left(3|b_c|^2 + 3\text{Tr}(Y_u Y_u^\dagger) + |a_c^1|^2 + \text{Tr}(Y_\nu Y_\nu^\dagger) \right) - 36\text{Tr}(Y_d Y_d^\dagger Y_d Y_d^\dagger) \\
 & - 12\text{Tr}(Y_d Y_d^\dagger Y_u Y_u^\dagger) - 12\text{Tr}(Y_e Y_e^\dagger Y_e Y_e^\dagger) - 4\text{Tr}(Y_e Y_e^\dagger Y_\nu Y_\nu^\dagger) \tag{A.63}
 \end{aligned}$$

$$\gamma_{\hat{H}_u}^{(1)} = 3\text{Tr}(Y_u Y_u^\dagger) - \frac{1}{2}g_R^2 + \frac{3}{2}|b|^2 - \frac{3}{2}g_L^2 + |b_c|^2 + \text{Tr}(Y_\nu Y_\nu^\dagger) \tag{A.64}$$

$$\begin{aligned}
 \gamma_{\hat{H}_u}^{(2)} = & \frac{1}{4} \left(27g_L^4 + 6g_L^2 g_R^2 + 19g_R^4 \right. \\
 & + |b|^2 \left(-18\text{Tr}(Y_d Y_d^\dagger) - 15|b|^2 - 19|b_c|^2 + 24g_L^2 - 6\text{Tr}(Y_e Y_e^\dagger) \right) \\
 & - 4|b_c|^2 \left(3|b_c|^2 + 3\text{Tr}(Y_d Y_d^\dagger) + |a_c^1|^2 + \text{Tr}(Y_e Y_e^\dagger) \right) + 2 \left(32g_3^2 + g_{\text{BL}}^2 \right) \text{Tr}(Y_u Y_u^\dagger) \\
 & + 6g_{\text{BL}}^2 \text{Tr}(Y_\nu Y_\nu^\dagger) - 4\text{Tr}(f_c^1 f_c^{1\dagger} Y_\nu^T Y_\nu^*) - 4\text{Tr}(f_c^1 Y_\nu^\dagger Y_\nu f_c^{1\dagger}) - 12\text{Tr}(Y_d Y_d^\dagger Y_u Y_u^\dagger) \\
 & - 4\text{Tr}(Y_e Y_e^\dagger Y_\nu Y_\nu^\dagger) - 36\text{Tr}(Y_u Y_u^\dagger Y_u Y_u^\dagger) - 4\text{Tr}(Y_\nu f_c^{1\dagger} f_c^{1T} Y_\nu^\dagger) \\
 & \left. - 12\text{Tr}(Y_\nu Y_\nu^\dagger Y_\nu Y_\nu^\dagger) - 4\text{Tr}(f_c^{1\dagger} Y_\nu^T Y_\nu^* f_c^{1T}) \right) \tag{A.65}
 \end{aligned}$$

$$\gamma_{\hat{\Delta}^{c0}}^{(1)} = -2g_R^2 - 3g_{\text{BL}}^2 + |a_c^1|^2 + \text{Tr}(f_c^1 f_c^{1\dagger}) + \text{Tr}(f_c^{1\dagger} f_c^{1T}) \tag{A.66}$$

$$\begin{aligned}
 \gamma_{\hat{\Delta}^{c0}}^{(2)} = & \frac{1}{2} \left(72g_{\text{BL}}^4 + 24g_{\text{BL}}^2 g_R^2 + 44g_R^4 - 4|a_c^1|^2 \left(|a_c^1|^2 + |b_c|^2 \right) \right. \\
 & - \left(2g_R^2 + 3g_{\text{BL}}^2 \right) \left(\text{Tr}(f_c^1 f_c^{1\dagger}) + \text{Tr}(f_c^{1\dagger} f_c^{1T}) \right) - 4\text{Tr}(f_c^1 f_c^{1\dagger} f_c^1 f_c^{1\dagger}) \\
 & - 8\text{Tr}(f_c^1 f_c^{1\dagger} f_c^{1T} f_c^{1\dagger}) - 8\text{Tr}(f_c^1 f_c^{1\dagger} f_c^{1T} f_c^{1*}) - 4\text{Tr}(f_c^1 f_c^{1\dagger} Y_\nu^T Y_\nu^*) \\
 & - 4\text{Tr}(f_c^1 Y_\nu^\dagger Y_\nu f_c^{1\dagger}) - 4\text{Tr}(Y_\nu f_c^{1\dagger} f_c^{1T} Y_\nu^\dagger) - 4\text{Tr}(f_c^{1\dagger} f_c^{1T} f_c^{1\dagger} f_c^{1T}) \\
 & \left. - 8\text{Tr}(f_c^{1\dagger} f_c^{1T} f_c^{1*} f_c^{1T}) - 4\text{Tr}(f_c^{1\dagger} Y_\nu^T Y_\nu^* f_c^{1T}) \right) \tag{A.67}
 \end{aligned}$$

$$\gamma_{\hat{\Delta}^{c0}}^{(1)} = -2g_R^2 - 3g_{\text{BL}}^2 + |a_c^1|^2 \tag{A.68}$$

$$\begin{aligned}
 \gamma_{\hat{\Delta}^{c0}}^{(2)} = & 12g_{\text{BL}}^2 g_R^2 + 22g_R^4 + 36g_{\text{BL}}^4 \\
 & - |a_c^1|^2 \left(2|a_c^1|^2 + 2|b_c|^2 + \text{Tr}(f_c^1 f_c^{1\dagger}) + \text{Tr}(f_c^{1\dagger} f_c^{1T}) \right) \tag{A.69}
 \end{aligned}$$

$$\gamma_{\hat{\Omega}}^{(1)} = -4g_L^2 + |b|^2 \tag{A.70}$$

$$\begin{aligned}
 \gamma_{\hat{\Omega}}^{(2)} = & 28g_L^4 - |b|^2 \left(2|b_c|^2 + 3|b|^2 + 3\text{Tr}(Y_d Y_d^\dagger) + 3\text{Tr}(Y_u Y_u^\dagger) \right) \\
 & - g_R^2 + g_L^2 + \text{Tr}(Y_e Y_e^\dagger) + \text{Tr}(Y_\nu Y_\nu^\dagger) \tag{A.71}
 \end{aligned}$$

$$\gamma_{\hat{\Omega}^{c0}}^{(1)} = 2|b_c|^2 + |a_c^1|^2 \tag{A.72}$$

$$\begin{aligned}
 \gamma_{\hat{\Omega}^{c0}}^{(2)} = & -2|a_c^1|^4 - |a_c^1|^2 \left(-4g_R^2 - 6g_{\text{BL}}^2 + \text{Tr}(f_c^1 f_c^{1\dagger}) + \text{Tr}(f_c^{1\dagger} f_c^{1T}) \right) \\
 & - 2|b_c|^2 \left(2|b_c|^2 + 3|b|^2 - 3g_L^2 + 3\text{Tr}(Y_d Y_d^\dagger) + 3\text{Tr}(Y_u Y_u^\dagger) \right) \\
 & - g_R^2 + \text{Tr}(Y_e Y_e^\dagger) + \text{Tr}(Y_\nu Y_\nu^\dagger) \tag{A.73}
 \end{aligned}$$

In these expressions we have defined

$$F_c = f_c^1 f_c^{1\dagger} + f_c^1 f_c^{1*} + f_c^{1T} f_c^{1\dagger} + f_c^{1T} f_c^{1*} \quad (\text{A.74})$$

A.3.2 Beta functions for soft breaking masses of sleptons

Again, the results for the slepton soft SUSY breaking masses at 1-loop are shown. The beta functions read

$$16\pi^2 \frac{d}{dt} m_L^2 = 2Y_e m_{e^c}^2 Y_e^\dagger + 2m_{H_d}^2 Y_e Y_e^\dagger + 2m_{H_u}^2 Y_\nu Y_\nu^\dagger + m_L^2 Y_e Y_e^\dagger + Y_e Y_e^\dagger m_L^2 + m_L^2 Y_\nu Y_\nu^\dagger + Y_\nu Y_\nu^\dagger m_L^2 + 2Y_\nu m_{\nu^c}^2 Y_\nu^\dagger + 2T_e T_e^\dagger + 2T_\nu T_\nu^\dagger - \left(3g_{\text{BL}}^2 |M_1|^2 + 6g_L^2 |M_L|^2 + \frac{3}{4}g_{\text{BL}}^2 S_2 \right) \mathbf{1} \quad (\text{A.75})$$

$$16\pi^2 \frac{d}{dt} m_{e^c}^2 = 2Y_e^\dagger Y_e m_{e^c}^2 + 2m_{e^c}^2 Y_e^\dagger Y_e + 4m_{H_d}^2 Y_e^\dagger Y_e + 4Y_e^\dagger m_L^2 Y_e + 4T_e^\dagger T_e - \left(3g_{\text{BL}}^2 |M_1|^2 + 2g_R^2 |M_R|^2 - \frac{3}{4}g_{\text{BL}}^2 S_2 - \frac{1}{2}g_R^2 S_3 \right) \mathbf{1} \quad (\text{A.76})$$

where

$$S_2 = 2(m_{\Delta_{c0}}^2 - m_{\bar{\Delta}_{c0}}^2) + \text{Tr} [m_{d^c}^2 - m_{e^c}^2 + m_{u^c}^2 - m_{\nu^c}^2 + 2m_L^2 - 2m_Q^2] \quad (\text{A.77})$$

$$S_3 = 2(m_{\Delta_{c0}}^2 - m_{\bar{\Delta}_{c0}}^2 - m_{H_d}^2 + m_{H_u}^2) + \text{Tr} [3m_{d^c}^2 + m_{e^c}^2 - 3m_{u^c}^2 - m_{\nu^c}^2] \quad (\text{A.78})$$

A.3.3 Beta functions for gauge couplings

$$\beta_{g_{\text{BL}}}^{(1)} = 9g_{\text{BL}}^3 \quad (\text{A.79})$$

$$\beta_{g_{\text{BL}}}^{(2)} = \frac{1}{2}g_{\text{BL}}^3 \left(16g_3^2 + 50g_{\text{BL}}^2 + 18g_L^2 + 30g_R^2 - 12|a_c^1|^2 - 9\text{Tr}(f_c^1 f_c^{1\dagger}) - 2\text{Tr}(Y_d Y_d^\dagger) - 6\text{Tr}(Y_e Y_e^\dagger) - 2\text{Tr}(Y_u Y_u^\dagger) - 6\text{Tr}(Y_\nu Y_\nu^\dagger) - 9\text{Tr}(f_c^{1\dagger} f_c^{1T}) \right) \quad (\text{A.80})$$

$$\beta_{g_L}^{(1)} = 3g_L^3 \quad (\text{A.81})$$

$$\beta_{g_L}^{(2)} = \frac{1}{3}g_L^3 \left(-28|b|^2 + 3(24g_3^2 - 2|b_c|^2 - 2\text{Tr}(Y_e Y_e^\dagger) - 2\text{Tr}(Y_\nu Y_\nu^\dagger) + 3g_{\text{BL}}^2 + 49g_L^2 - 6\text{Tr}(Y_d Y_d^\dagger) - 6\text{Tr}(Y_u Y_u^\dagger) + g_R^2) \right) \quad (\text{A.82})$$

$$\beta_{g_R}^{(1)} = 9g_R^3 \quad (\text{A.83})$$

$$\beta_{g_R}^{(2)} = g_R^3 \left(24g_3^2 + 15g_{\text{BL}}^2 + 3g_L^2 + 15g_R^2 - 4|a_c^1|^2 - 4|b|^2 - 2|b_c|^2 - 3\text{Tr}(f_c^1 f_c^{1\dagger}) - 6\text{Tr}(Y_d Y_d^\dagger) - 2\text{Tr}(Y_e Y_e^\dagger) - 6\text{Tr}(Y_u Y_u^\dagger) - 2\text{Tr}(Y_\nu Y_\nu^\dagger) - 3\text{Tr}(f_c^{1\dagger} f_c^{1T}) \right) \quad (\text{A.84})$$

$$\beta_{g_3}^{(1)} = -3g_3^3 \quad (\text{A.85})$$

$$\beta_{g_3}^{(2)} = g_3^3 \left(14g_3^2 + 3g_R^2 - 4\text{Tr}(Y_d Y_d^\dagger) - 4\text{Tr}(Y_u Y_u^\dagger) + 9g_L^2 + g_{\text{BL}}^2 \right) \quad (\text{A.86})$$

References

- [1] P. Minkowski, $\mu \rightarrow e\gamma$ at a rate of one out of 1-billion muon decays?, *Phys. Lett. B* **67** (1977) 421 [SPIRES].

- [2] T. Yanagida, *Horizontal symmetry and masses of neutrinos*, in *KEK lectures*, O. Sawada and A. Sugamoto eds., KEK, Tsukuba Japan (1979) [[SPIRES](#)].
- [3] M. Gell-Mann, P. Ramond and R. Slansky, *Complex spinors and unified theories*, in *Supergravity*, P. van Nieuwenhuizen and D. Freedman eds., North Holland, Amsterdam The Netherlands (1979) [[SPIRES](#)].
- [4] R.N. Mohapatra and G. Senjanović, *Neutrino mass and spontaneous parity nonconservation*, *Phys. Rev. Lett.* **44** (1980) 912 [[SPIRES](#)].
- [5] J. Schechter and J.W.F. Valle, *Neutrino masses in $SU(2) \times U(1)$ theories*, *Phys. Rev. D* **22** (1980) 2227 [[SPIRES](#)].
- [6] T.P. Cheng and L.-F. Li, *Neutrino masses, mixings and oscillations in $SU(2) \times U(1)$ models of electroweak interactions*, *Phys. Rev. D* **22** (1980) 2860 [[SPIRES](#)].
- [7] SUPER-KAMIOKANDE collaboration, Y. Fukuda et al., *Evidence for oscillation of atmospheric neutrinos*, *Phys. Rev. Lett.* **81** (1998) 1562 [[hep-ex/9807003](#)] [[SPIRES](#)].
- [8] SNO collaboration, Q.R. Ahmad et al., *Direct evidence for neutrino flavor transformation from neutral-current interactions in the Sudbury Neutrino Observatory*, *Phys. Rev. Lett.* **89** (2002) 011301 [[nucl-ex/0204008](#)] [[SPIRES](#)].
- [9] KAMLAND collaboration, K. Eguchi et al., *First results from KamLAND: evidence for reactor anti-neutrino disappearance*, *Phys. Rev. Lett.* **90** (2003) 021802 [[hep-ex/0212021](#)] [[SPIRES](#)].
- [10] E. Ma, *Pathways to naturally small neutrino masses*, *Phys. Rev. Lett.* **81** (1998) 1171 [[hep-ph/9805219](#)] [[SPIRES](#)].
- [11] R. Foot, H. Lew, X.G. He and G.C. Joshi, *Seesaw neutrino masses induced by a triplet of leptons*, *Z. Phys. C* **44** (1989) 441 [[SPIRES](#)].
- [12] F. Borzumati and A. Masiero, *Large muon and electron number violations in supergravity theories*, *Phys. Rev. Lett.* **57** (1986) 961 [[SPIRES](#)].
- [13] J. Hisano, T. Moroi, K. Tobe, M. Yamaguchi and T. Yanagida, *Lepton flavor violation in the supersymmetric standard model with seesaw induced neutrino masses*, *Phys. Lett. B* **357** (1995) 579 [[hep-ph/9501407](#)] [[SPIRES](#)].
- [14] J. Hisano, T. Moroi, K. Tobe and M. Yamaguchi, *Lepton-flavor violation via right-handed neutrino Yukawa couplings in supersymmetric standard model*, *Phys. Rev. D* **53** (1996) 2442 [[hep-ph/9510309](#)] [[SPIRES](#)].
- [15] J.R. Ellis, J. Hisano, M. Raidal and Y. Shimizu, *A new parametrization of the seesaw mechanism and applications in supersymmetric models*, *Phys. Rev. D* **66** (2002) 115013 [[hep-ph/0206110](#)] [[SPIRES](#)].
- [16] F. Deppisch, H. Pas, A. Redelbach, R. Ruckl and Y. Shimizu, *Probing the Majorana mass scale of right-handed neutrinos in $mSUGRA$* , *Eur. Phys. J. C* **28** (2003) 365 [[hep-ph/0206122](#)] [[SPIRES](#)].
- [17] S.T. Petcov, S. Profumo, Y. Takanishi and C.E. Yaguna, *Charged lepton flavor violating decays: leading logarithmic approximation versus full RG results*, *Nucl. Phys. B* **676** (2004) 453 [[hep-ph/0306195](#)] [[SPIRES](#)].
- [18] E. Arganda and M.J. Herrero, *Testing supersymmetry with lepton flavor violating τ and μ decays*, *Phys. Rev. D* **73** (2006) 055003 [[hep-ph/0510405](#)] [[SPIRES](#)].

- [19] S.T. Petcov, T. Shindou and Y. Takanishi, *Majorana CP-violating phases, RG running of neutrino mixing parameters and charged lepton flavour violating decays*, *Nucl. Phys. B* **738** (2006) 219 [[hep-ph/0508243](#)] [[SPIRES](#)].
- [20] S. Antusch, E. Arganda, M.J. Herrero and A.M. Teixeira, *Impact of θ_{13} on lepton flavour violating processes within SUSY seesaw*, *JHEP* **11** (2006) 090 [[hep-ph/0607263](#)] [[SPIRES](#)].
- [21] F. Deppisch and J.W.F. Valle, *Enhanced lepton flavour violation in the supersymmetric inverse seesaw model*, *Phys. Rev. D* **72** (2005) 036001 [[hep-ph/0406040](#)] [[SPIRES](#)].
- [22] M. Hirsch, J.W.F. Valle, W. Porod, J.C. Romao and A. Villanova del Moral, *Probing minimal supergravity in type-I seesaw with lepton flavour violation at the LHC*, *Phys. Rev. D* **78** (2008) 013006 [[arXiv:0804.4072](#)] [[SPIRES](#)].
- [23] E. Arganda, M.J. Herrero and A.M. Teixeira, *$\mu - e$ conversion in nuclei within the CMSSM seesaw: universality versus non-universality*, *JHEP* **10** (2007) 104 [[arXiv:0707.2955](#)] [[SPIRES](#)].
- [24] F. Deppisch, T.S. Kosmas and J.W.F. Valle, *Enhanced $\mu^- - e^-$ conversion in nuclei in the inverse seesaw model*, *Nucl. Phys. B* **752** (2006) 80 [[hep-ph/0512360](#)] [[SPIRES](#)].
- [25] A. Rossi, *Supersymmetric seesaw without singlet neutrinos: neutrino masses and lepton-flavour violation*, *Phys. Rev. D* **66** (2002) 075003 [[hep-ph/0207006](#)] [[SPIRES](#)].
- [26] M. Hirsch, S. Kaneko and W. Porod, *Supersymmetric seesaw type-II: LHC and lepton flavour violating phenomenology*, *Phys. Rev. D* **78** (2008) 093004 [[arXiv:0806.3361](#)] [[SPIRES](#)].
- [27] J.N. Esteves, M. Hirsch, W. Porod, J.C. Romao and F. Staub, *Supersymmetric type-III seesaw: lepton flavour violating decays and dark matter*, [arXiv:1010.6000](#) [[SPIRES](#)].
- [28] J. Hisano, M.M. Nojiri, Y. Shimizu and M. Tanaka, *Lepton flavor violation in the left-handed slepton production at future lepton colliders*, *Phys. Rev. D* **60** (1999) 055008 [[hep-ph/9808410](#)] [[SPIRES](#)].
- [29] J.N. Esteves et al., *Flavour violation at the LHC: type-I versus type-II seesaw in minimal supergravity*, *JHEP* **05** (2009) 003 [[arXiv:0903.1408](#)] [[SPIRES](#)].
- [30] G.A. Blair, W. Porod and P.M. Zerwas, *The reconstruction of supersymmetric theories at high energy scales*, *Eur. Phys. J. C* **27** (2003) 263 [[hep-ph/0210058](#)] [[SPIRES](#)].
- [31] A. Freitas, W. Porod and P.M. Zerwas, *Determining sneutrino masses and physical implications*, *Phys. Rev. D* **72** (2005) 115002 [[hep-ph/0509056](#)] [[SPIRES](#)].
- [32] F. Deppisch, A. Freitas, W. Porod and P.M. Zerwas, *Determining heavy mass parameters in supersymmetric SO(10) models*, *Phys. Rev. D* **77** (2008) 075009 [[arXiv:0712.0361](#)] [[SPIRES](#)].
- [33] M.R. Buckley and H. Murayama, *How can we test seesaw experimentally?*, *Phys. Rev. Lett.* **97** (2006) 231801 [[hep-ph/0606088](#)] [[SPIRES](#)].
- [34] B.C. Allanach, J.P. Conlon and C.G. Lester, *Measuring smuon-selectron mass splitting at the CERN LHC and patterns of supersymmetry breaking*, *Phys. Rev. D* **77** (2008) 076006 [[arXiv:0801.3666](#)] [[SPIRES](#)].
- [35] A. Abada, A.J.R. Figueiredo, J.C. Romao and A.M. Teixeira, *Interplay of LFV and slepton mass splittings at the LHC as a probe of the SUSY seesaw*, *JHEP* **10** (2010) 104 [[arXiv:1007.4833](#)] [[SPIRES](#)].

- [36] J.C. Pati and A. Salam, *Lepton number as the fourth color*, *Phys. Rev. D* **10** (1974) 275 [Erratum *ibid.* **D 11** (1975) 703] [SPIRES].
- [37] R.N. Mohapatra and J.C. Pati, *A natural left-right symmetry*, *Phys. Rev. D* **11** (1975) 2558 [SPIRES].
- [38] G. Senjanović and R.N. Mohapatra, *Exact left-right symmetry and spontaneous violation of parity*, *Phys. Rev. D* **12** (1975) 1502 [SPIRES].
- [39] H. Georgi, *The state of the art — gauge theories* (Talk), *AIP Conf. Proc.* **23** (1975) 575 [SPIRES].
- [40] H. Fritzsch and P. Minkowski, *Unified interactions of leptons and hadrons*, *Annals Phys.* **93** (1975) 193 [SPIRES].
- [41] R.N. Mohapatra and A. Rasin, *A supersymmetric solution to CP problems*, *Phys. Rev. D* **54** (1996) 5835 [hep-ph/9604445] [SPIRES].
- [42] R.N. Mohapatra, *New contributions to neutrinoless double- β decay in supersymmetric theories*, *Phys. Rev. D* **34** (1986) 3457 [SPIRES].
- [43] S.P. Martin, *Some simple criteria for gauged R-parity*, *Phys. Rev. D* **46** (1992) 2769 [hep-ph/9207218] [SPIRES].
- [44] M. Malinsky, J.C. Romao and J.W.F. Valle, *Novel supersymmetric SO(10) seesaw mechanism*, *Phys. Rev. Lett.* **95** (2005) 161801 [hep-ph/0506296] [SPIRES].
- [45] M. Cvetič and J.C. Pati, *$N = 1$ supergravity within the minimal left-right symmetric model*, *Phys. Lett. B* **135** (1984) 57 [SPIRES].
- [46] E.K. Akhmedov and M. Frigerio, *Interplay of type-I and type-II seesaw contributions to neutrino mass*, *JHEP* **01** (2007) 043 [hep-ph/0609046] [SPIRES].
- [47] R. Kuchimanchi and R.N. Mohapatra, *No parity violation without R-parity violation*, *Phys. Rev. D* **48** (1993) 4352 [hep-ph/9306290] [SPIRES].
- [48] K.S. Babu and R.N. Mohapatra, *Minimal supersymmetric left-right model*, *Phys. Lett. B* **668** (2008) 404 [arXiv:0807.0481] [SPIRES].
- [49] R. Kuchimanchi and R.N. Mohapatra, *Upper bound on the W_R mass in automatically R-conserving SUSY models*, *Phys. Rev. Lett.* **75** (1995) 3989 [hep-ph/9509256] [SPIRES].
- [50] C.S. Aulakh, K. Benakli and G. Senjanović, *Reconciling supersymmetry and left-right symmetry*, *Phys. Rev. Lett.* **79** (1997) 2188 [hep-ph/9703434] [SPIRES].
- [51] C.S. Aulakh, A. Melfo, A. Rasin and G. Senjanović, *Supersymmetry and large scale left-right symmetry*, *Phys. Rev. D* **58** (1998) 115007 [hep-ph/9712551] [SPIRES].
- [52] M.J. Hayashi and A. Murayama, *Radiative breaking of $SU(2)_R \times U(1)_{(B-L)}$ gauge symmetry induced by broken $N = 1$ supergravity in a left-right symmetric model*, *Phys. Lett. B* **153** (1985) 251 [SPIRES].
- [53] P. Fileviez Perez and S. Spinner, *Spontaneous R-parity breaking and left-right symmetry*, *Phys. Lett. B* **673** (2009) 251 [arXiv:0811.3424] [SPIRES].
- [54] N. Setzer and S. Spinner, *One-loop RGEs for two left-right SUSY models*, *Phys. Rev. D* **71** (2005) 115010 [hep-ph/0503244] [SPIRES].
- [55] W. Chao, *Neutrino masses and lepton-flavor-violating τ decays in the supersymmetric left-right model*, arXiv:0705.4351 [SPIRES].

- [56] R. Barbieri and L.J. Hall, *Signals for supersymmetric unification*, *Phys. Lett. B* **338** (1994) 212 [[hep-ph/9408406](#)] [[SPIRES](#)].
- [57] S.P. Martin and M.T. Vaughn, *Two loop renormalization group equations for soft supersymmetry breaking couplings*, *Phys. Rev. D* **50** (1994) 2282 [*Erratum ibid.* **D 78** (2008) 039903] [[hep-ph/9311340](#)] [[SPIRES](#)].
- [58] F. Staub, *SARAH*, [arXiv:0806.0538](#) [[SPIRES](#)].
- [59] F. Staub, *From superpotential to model files for FeynArts and CalcHep/CompHEP*, *Comput. Phys. Commun.* **181** (2010) 1077 [[arXiv:0909.2863](#)] [[SPIRES](#)].
- [60] F. Staub, *Automatic calculation of supersymmetric renormalization group equations and self energies*, [arXiv:1002.0840](#) [[SPIRES](#)].
- [61] *SARAH supplementary data homepage*, <http://theorie.physik.uni-wuerzburg.de/~fnst Staub/supplementary.html>.
- [62] W. Porod, *SPheno, a program for calculating supersymmetric spectra, SUSY particle decays and SUSY particle production at e^+e^- colliders*, *Comput. Phys. Commun.* **153** (2003) 275 [[hep-ph/0301101](#)] [[SPIRES](#)].
- [63] K.S. Babu, B. Dutta and R.N. Mohapatra, *Partial Yukawa unification and a supersymmetric origin of flavor mixing*, *Phys. Rev. D* **60** (1999) 095004 [[hep-ph/9812421](#)] [[SPIRES](#)].
- [64] T. Schwetz, M.A. Tortola and J.W.F. Valle, *Three-flavour neutrino oscillation update*, *New J. Phys.* **10** (2008) 113011 [[arXiv:0808.2016](#)] [[SPIRES](#)].
- [65] MINOS collaboration, *Preliminary results from MINOS on muon neutrino disappearance based on an exposure of 2.5×10^{20} 120 GeV protons on the NuMI target*, [arXiv:0708.1495](#) [[SPIRES](#)].
- [66] KAMLAND collaboration, S. Abe et al., *Precision measurement of neutrino oscillation parameters with KamLAND*, *Phys. Rev. Lett.* **100** (2008) 221803 [[arXiv:0801.4589](#)] [[SPIRES](#)].
- [67] P.F. Harrison, D.H. Perkins and W.G. Scott, *Tri-bimaximal mixing and the neutrino oscillation data*, *Phys. Lett. B* **530** (2002) 167 [[hep-ph/0202074](#)] [[SPIRES](#)].
- [68] K.S. Babu, B. Dutta and R.N. Mohapatra, *Lepton flavor violation and the origin of the seesaw mechanism*, *Phys. Rev. D* **67** (2003) 076006 [[hep-ph/0211068](#)] [[SPIRES](#)].
- [69] D.M. Pierce, J.A. Bagger, K.T. Matchev and R.-J. Zhang, *Precision corrections in the minimal supersymmetric standard model*, *Nucl. Phys. B* **491** (1997) 3 [[hep-ph/9606211](#)] [[SPIRES](#)].
- [70] L.J. Hall, *Grand unification of effective gauge theories*, *Nucl. Phys. B* **178** (1981) 75 [[SPIRES](#)].
- [71] J. Kopp, M. Lindner, V. Niro and T.E.J. Underwood, *On the consistency of perturbativity and gauge coupling unification*, *Phys. Rev. D* **81** (2010) 025008 [[arXiv:0909.2653](#)] [[SPIRES](#)].
- [72] S.K. Majee, M.K. Parida, A. Raychaudhuri and U. Sarkar, *Low intermediate scales for leptogenesis in supersymmetric SO(10) grand unified theories*, *Phys. Rev. D* **75** (2007) 075003 [[hep-ph/0701109](#)] [[SPIRES](#)].

- [73] W. Martens, L. Mihaila, J. Salomon and M. Steinhauser, *Minimal supersymmetric SU(5) and gauge coupling unification at three loops*, [arXiv:1008.3070](#) [SPIRES].
- [74] D. Borah and U.A. Yajnik, *Supersymmetric left-right models with gauge coupling unification and fermion mass universality*, [arXiv:1010.6289](#) [SPIRES].
- [75] J.A. Aguilar-Saavedra et al., *Supersymmetry parameter analysis: SPA convention and project*, *Eur. Phys. J. C* **46** (2006) 43 [[hep-ph/0511344](#)] [SPIRES].
- [76] B.C. Allanach et al., *The Snowmass points and slopes: benchmarks for SUSY searches*, in *Proc. of the APS/DPF/DPB Summer Study on the Future of Particle Physics (Snowmass 2001)*, Snowmass U.S.A. June 30– July 21 2001, N. Graf ed., [*Eur. Phys. J. C* **25** (2002) 113] [[hep-ph/0202233](#)] [SPIRES].
- [77] S.L. Glashow, J. Iliopoulos and L. Maiani, *Weak interactions with lepton-hadron symmetry*, *Phys. Rev. D* **2** (1970) 1285 [SPIRES].
- [78] MEG collaboration, *MEG: search for $\mu \rightarrow e\gamma$ down to 10^{-14} branching ratio*, proposal to PSI, Paul Scherrer Institute, Switzerland.
- [79] MEG collaboration, S. Mihara, *MEG experiment at the Paul Scherrer Institute*, *Nucl. Phys. A* **844** (2010) 150c [SPIRES].
- [80] Y. Kuno and Y. Okada, *Muon decay and physics beyond the standard model*, *Rev. Mod. Phys.* **73** (2001) 151 [[hep-ph/9909265](#)] [SPIRES].
- [81] Y. Okada, K.-I. Okumura and Y. Shimizu, *$\mu \rightarrow e\gamma$ and $\mu \rightarrow 3e$ processes with polarized muons and supersymmetric grand unified theories*, *Phys. Rev. D* **61** (2000) 094001 [[hep-ph/9906446](#)] [SPIRES].
- [82] J. Hisano, M. Nagai, P. Paradisi and Y. Shimizu, *Waiting for $\mu \rightarrow e\gamma$ from the MEG experiment*, *JHEP* **12** (2009) 030 [[arXiv:0904.2080](#)] [SPIRES].
- [83] I. Hinchliffe and F.E. Paige, *Lepton flavor violation at the LHC*, *Phys. Rev. D* **63** (2001) 115006 [[hep-ph/0010086](#)] [SPIRES].
- [84] D.F. Carvalho, J.R. Ellis, M.E. Gomez, S. Lola and J.C. Romao, *τ flavour violation in sparticle decays at the LHC*, *Phys. Lett. B* **618** (2005) 162 [[hep-ph/0206148](#)] [SPIRES].
- [85] E. Carquin, J. Ellis, M.E. Gomez, S. Lola and J. Rodriguez-Quintero, *Search for τ flavour violation at the LHC*, *JHEP* **05** (2009) 026 [[arXiv:0812.4243](#)] [SPIRES].
- [86] F.E. Paige, *Determining SUSY particle masses at LHC*, [hep-ph/9609373](#) [SPIRES].
- [87] I. Hinchliffe, F.E. Paige, M.D. Shapiro, J. Soderqvist and W. Yao, *Precision SUSY measurements at CERN LHC*, *Phys. Rev. D* **55** (1997) 5520 [[hep-ph/9610544](#)] [SPIRES].
- [88] H. Bachacou, I. Hinchliffe and F.E. Paige, *Measurements of masses in SUGRA models at CERN LHC*, *Phys. Rev. D* **62** (2000) 015009 [[hep-ph/9907518](#)] [SPIRES].
- [89] CMS collaboration, G.L. Bayatian et al., *CMS technical design report, volume II: physics performance*, *J. Phys. G* **34** (2007) 995 [SPIRES].
- [90] THE ATLAS collaboration, G. Aad et al., *Expected performance of the ATLAS experiment — detector, trigger and physics*, [arXiv:0901.0512](#) [SPIRES].
- [91] B.C. Allanach, C.G. Lester, M.A. Parker and B.R. Webber, *Measuring sparticle masses in non-universal string inspired models at the LHC*, *JHEP* **09** (2000) 004 [[hep-ph/0007009](#)] [SPIRES].

- [92] A. Bartl et al., *Test of lepton flavour violation at LHC*, *Eur. Phys. J. C* **46** (2006) 783 [[hep-ph/0510074](#)] [[SPIRES](#)].
- [93] A.J. Buras, L. Calibbi and P. Paradisi, *Slepton mass-splittings as a signal of LFV at the LHC*, *JHEP* **06** (2010) 042 [[arXiv:0912.1309](#)] [[SPIRES](#)].
- [94] Y.M. Andreev, S.I. Bitjukov, N.V. Krasnikov and A.N. Toropin, *Using the $e^\pm\mu^\mp + ET^{\text{miss}}$ signature in the search for supersymmetry and lepton flavour violation in neutralino decays*, *Phys. Atom. Nucl.* **70** (2007) 1717 [[hep-ph/0608176](#)] [[SPIRES](#)].
- [95] F. del Aguila et al., *Collider aspects of flavour physics at high Q* , *Eur. Phys. J. C* **57** (2008) 183 [[arXiv:0801.1800](#)] [[SPIRES](#)].
- [96] P.C. West, *The Yukawa β -function in $N = 1$ rigid supersymmetric theories*, *Phys. Lett. B* **137** (1984) 371 [[SPIRES](#)].
- [97] D.R.T. Jones and L. Mezincescu, *The chiral anomaly and a class of two loop finite supersymmetric gauge theories*, *Phys. Lett. B* **138** (1984) 293 [[SPIRES](#)].
- [98] I. Jack, D.R.T. Jones and A. Pickering, *Renormalisation invariance and the soft β -functions*, *Phys. Lett. B* **426** (1998) 73 [[hep-ph/9712542](#)] [[SPIRES](#)].
- [99] Y. Yamada, *Two loop renormalization group equations for soft SUSY breaking scalar interactions: supergraph method*, *Phys. Rev. D* **50** (1994) 3537 [[hep-ph/9401241](#)] [[SPIRES](#)].
- [100] I. Jack, D.R.T. Jones, S.P. Martin, M.T. Vaughn and Y. Yamada, *Decoupling of the ϵ scalar mass in softly broken supersymmetry*, *Phys. Rev. D* **50** (1994) 5481 [[hep-ph/9407291](#)] [[SPIRES](#)].
- [101] I. Jack, D.R.T. Jones and A. Pickering, *The soft scalar mass β -function*, *Phys. Lett. B* **432** (1998) 114 [[hep-ph/9803405](#)] [[SPIRES](#)].